

1
2
3
4
5
6
7
8
9
10
11
12
13
14
15
16
17
18
19
20
21
22
23
24
25
26
27
28
29

Supplementary Information

Surface Manipulation for Prevention of Migratory Viscous Crude Oil Fouling in Superhydrophilic Membranes

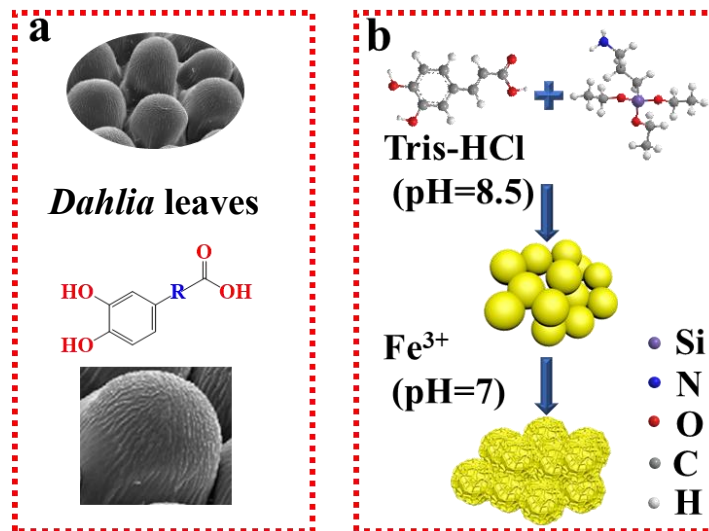
Yuanyuan Zhao^[a], Xiaobin Yang^[a], Zhongjun Cheng^[a], Cher Hon Lau^[b], Jun Ma^[c], Lu Shao^{[a]*}

^[a] MIIT Key Laboratory of Critical Materials Technology for New Energy Conversion and Storage, State Key Laboratory of Urban Water Resource and Environment, School of Chemistry and Chemical Engineering, Harbin Institute of Technology, Xidazhi 92, Harbin 150001, PR China

^[b] School of Engineering, The University of Edinburgh, The King's Buildings, Mayfield Road, EH9 3JL, United Kingdom

^[c] School of Environments; Harbin Institute of Technology; Harbin 150001, PR China

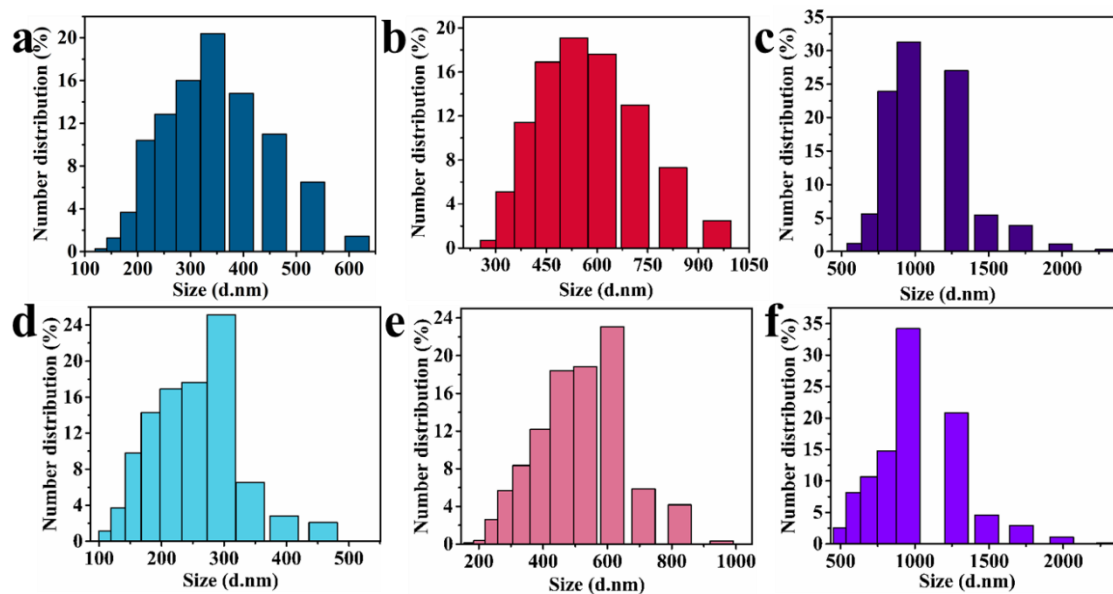
*e-mail: shaolu@hit.edu.cn



31

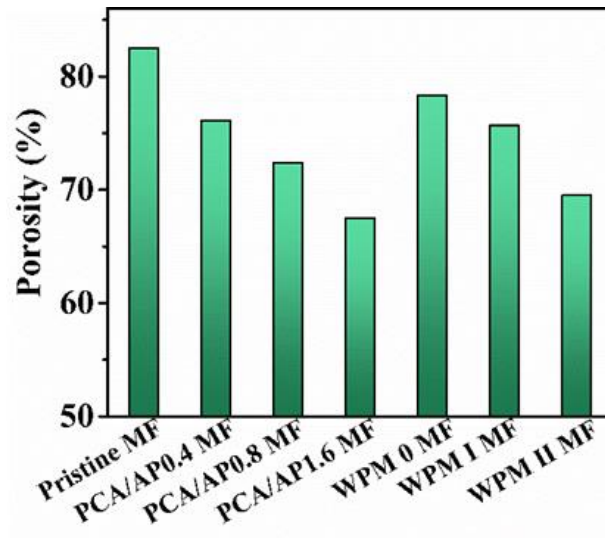
32 **Supplementary Figure 1|** (a) Structures of caffeoyl esters and flavonoids in *dahlia*
 33 leaves¹; (b) Synthesis of wrinkled patterns on smooth microparticles via a two-step
 34 process: 1) Synthesizing smooth hydrophilic microparticles. 2) Creating cuticle-like
 35 nanostructures on microparticles surfaces via microparticles and Fe^{3+} coordination.

36



37

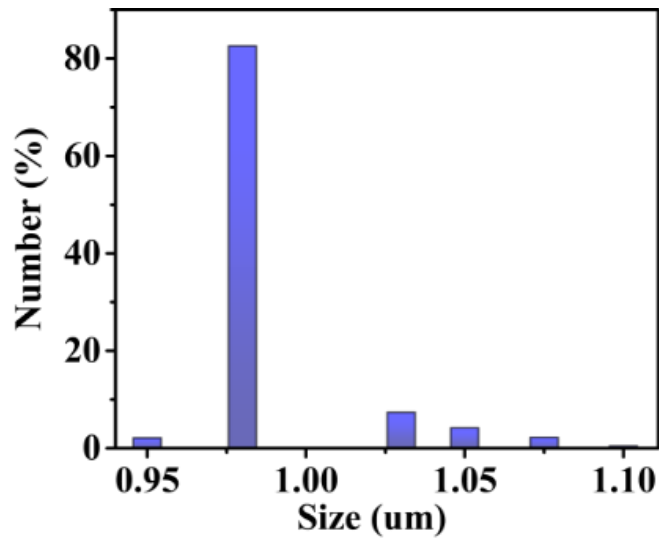
38 **Supplementary Figure 2|** The responding size distribution of microparticles of (a)
 39 PCA/AP0.4; (b) PCA/AP0.8; (c) PCA/AP1.6; (d) WPM 0; (e) WPM I; (f) WPM II.



40

41 **Supplementary Figure 3|** (a) The porosity of the membranes.

42



43

44 **Supplementary Figure 4|** The responding pore size distribution of the pristine MF.

45

46

47

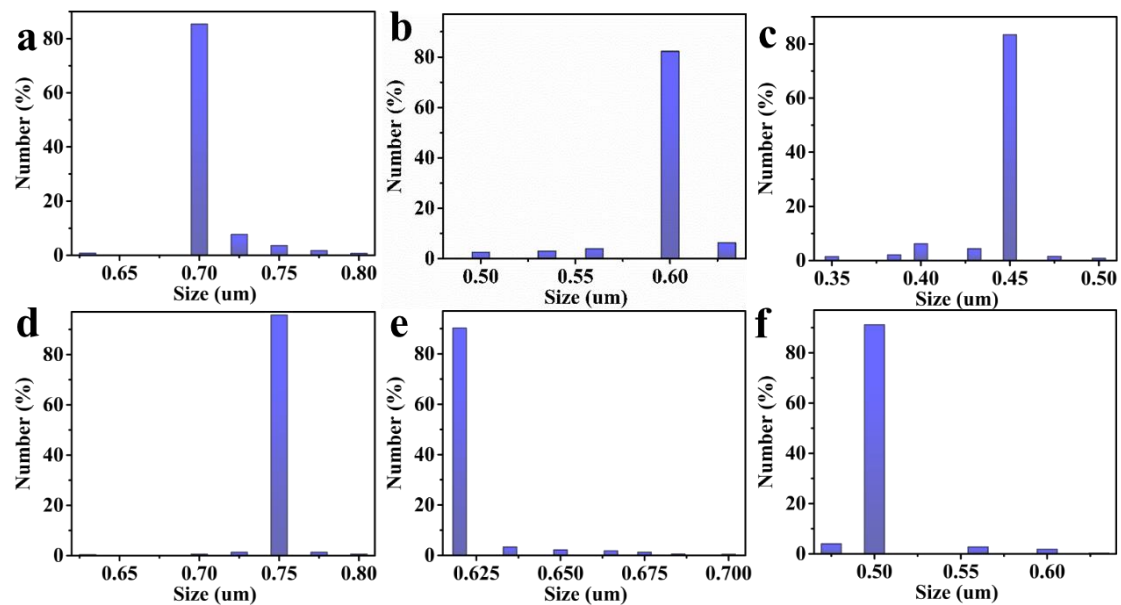
48

49

50

51

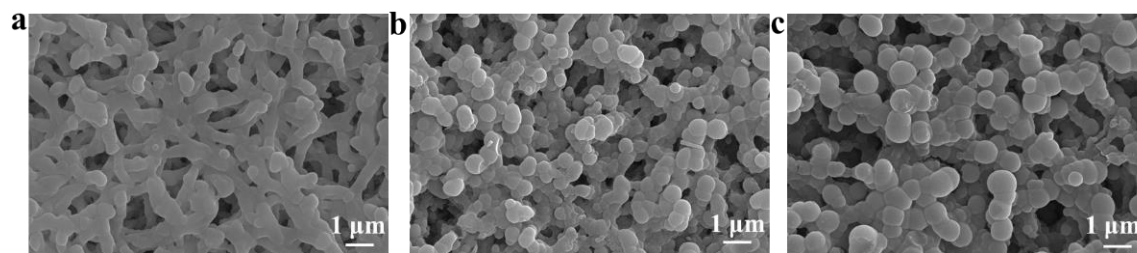
52



53

54 **Supplementary Figure 5** | The responding pore size distribution of (a) PCA/AP0.4; (b)
 55 PCA/AP0.8; (c) PCA/AP1.6; (d) WPM 0; (e) WPM I; (f) WPM II MF.

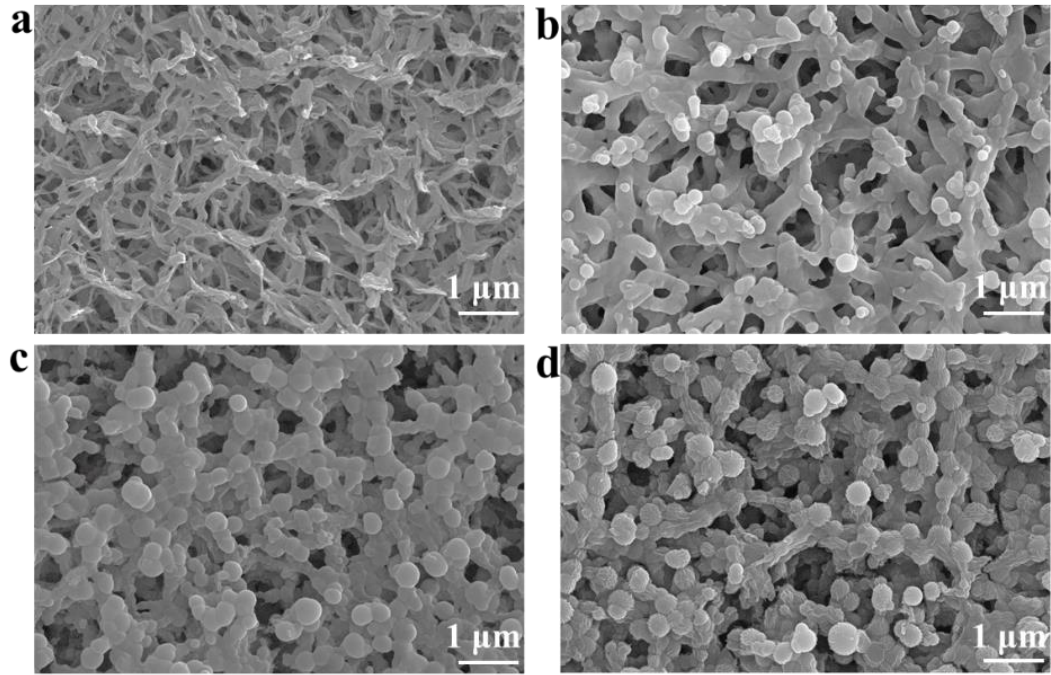
56



57

58 **Supplementary Figure 6** | SEM images of the surface of (a) PCA/AP0.4; (b)
 59 PCA/AP0.8; (c) PCA/AP1.6 MF.

60

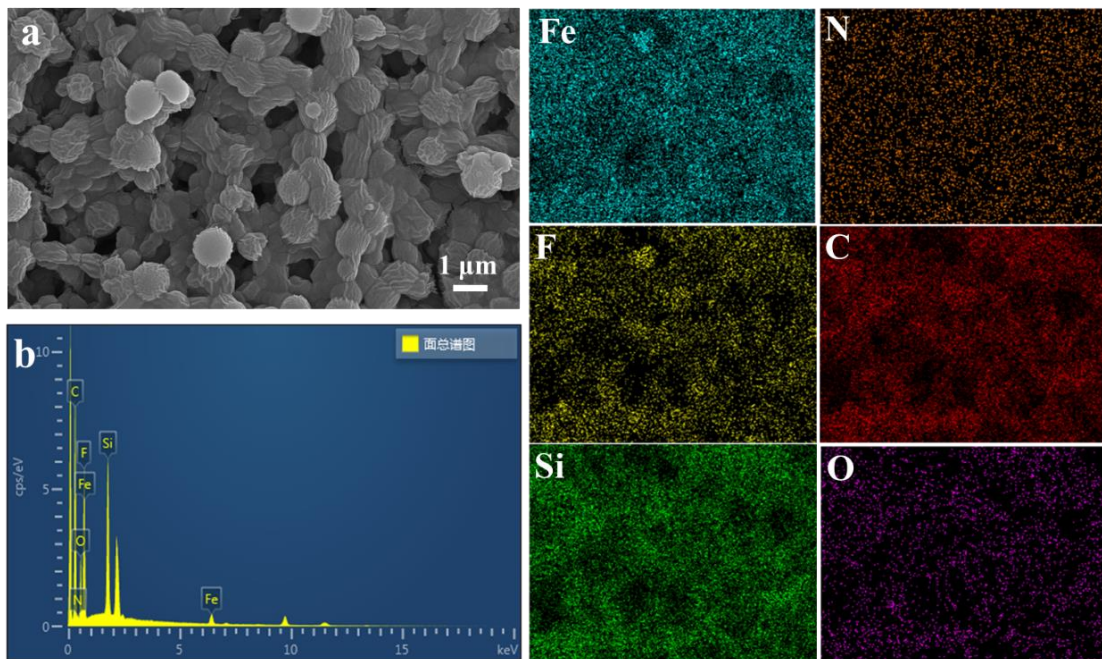


61

62 **Supplementary Figure 7** | (a-d) SEM images of the pristine MF, WPM 0, WPM I, and

63 WPM II MF.

64



65

66 **Supplementary Figure 8** | (a) SEM images; (b) Corresponding EDS mapping of the

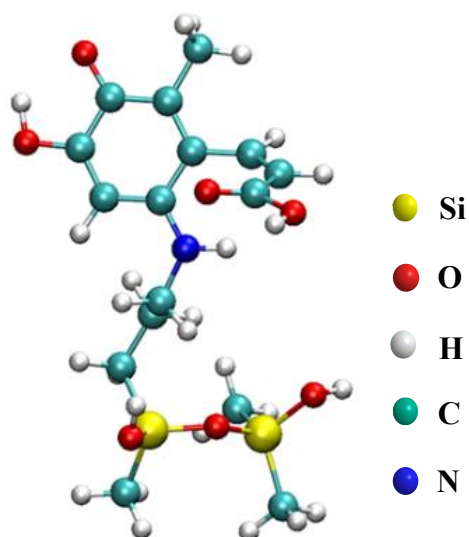
67 WPM II MF.

68 Compared with the typical fibrous membrane pore structure of the pristine MF, the pore

69 size and porosity of PCA/AP MFs decreased with the increase of the APTES content,

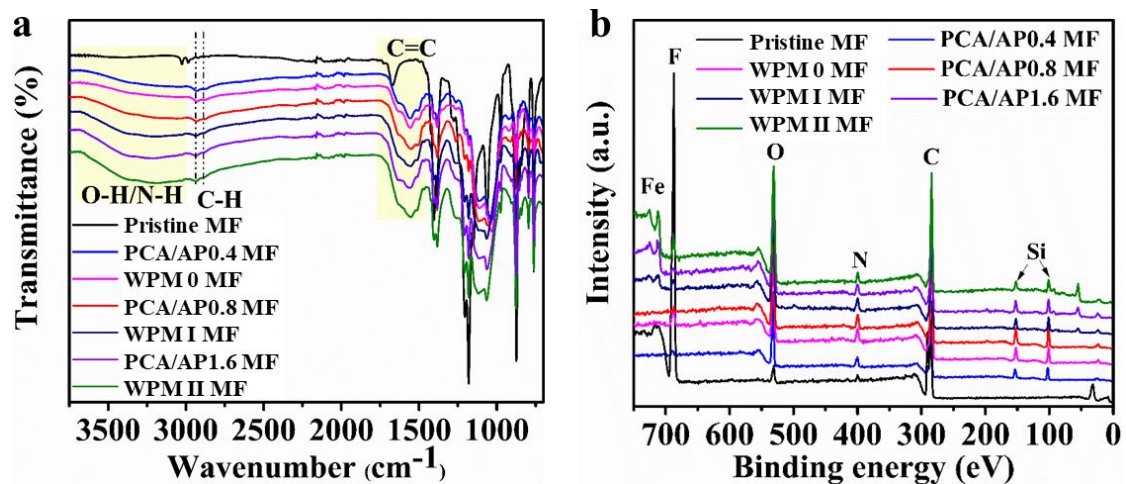
70 which was mainly due to the deposition of gradual increase PCA/AP microparticles on
71 the surface of the membrane. While, the pore size and porosity of each WPM MFs had
72 a weak upward trend compared to the corresponding PCA/AP MFs, which was mainly
73 due to the deformation of the microparticles surface after Fe³⁺ modification. The pore
74 size of WPM 0 MF (0.75 μm) increased 7.1% than that of PCA/AP0.4. The pore size
75 of WPM I MF (0.625 μm) increased 4.1% than that of PCA/AP0.8 and the pore size of
76 WPM II MF (0.5 μm) increased 11.1% than that of PCA/AP1.6. This varying degree of
77 wrinkling reduced the space for microparticles to be coated on WPM MFs surface
78 resulting in the pore size and porosity of WPM MFs would have a weak increase, which
79 also can be confirmed by SEM image of each membrane in Supplementary Figs. 6 and
80 7. The results of SEM images and corresponding EDS mapping of the membrane in
81 Supplementary Fig. 8 showed that we chose the synthesis process of the membranes
82 has been shaken in a water bath to ensure more uniform distribution of microparticles
83 on the membrane surface.

84



86 **Supplementary Figure 9** | Optimized geometry of PCA/AP.

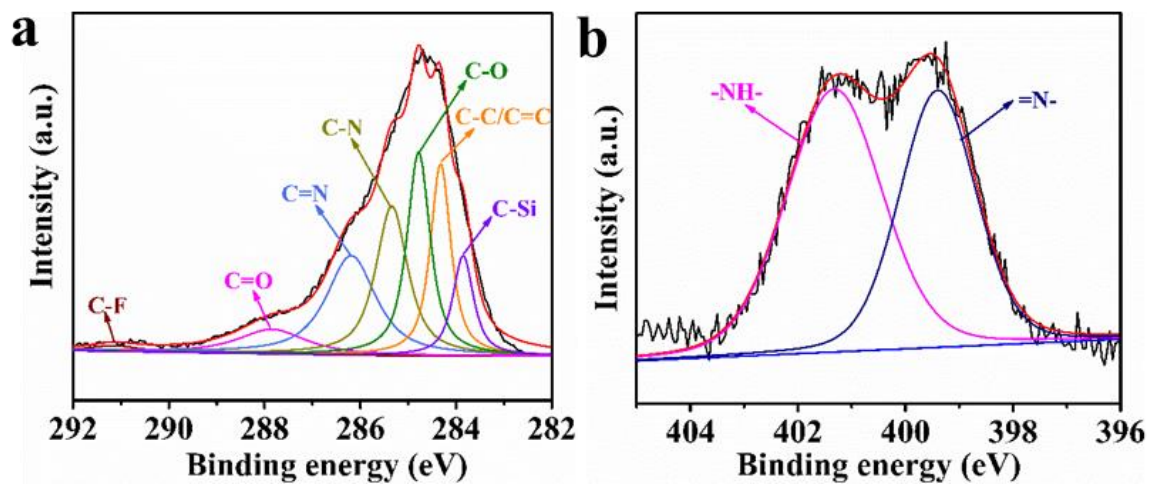
87



88

89 **Supplementary Figure 10|** (a) FTIR spectra and (b) XPS spectra of all membranes.

90



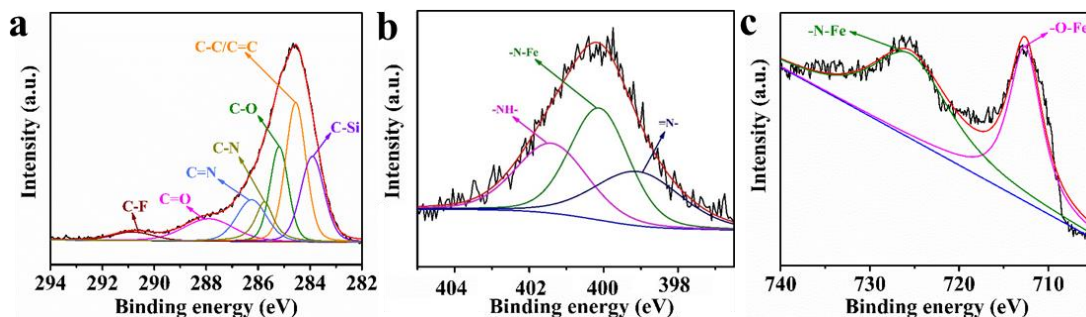
91

92 **Supplementary Figure 11|** The C 1s and N 1s spectrum of PCA/AP1.6 MF.

93 The wide absorption peak at 3000-3500 cm^{-1} were attributed to the stretching of O-
 94 H/N-H in the phenolic hydroxyl group/amino group of the modification membranes.

95 The broad absorption band at 1650 cm^{-1} was assigned to benzene ring C=C of PCA, as
 96 well as, the new peaks at 1125 and 910 cm^{-1} were corresponding to Si-O-Si and Si-OH,
 97 respectively

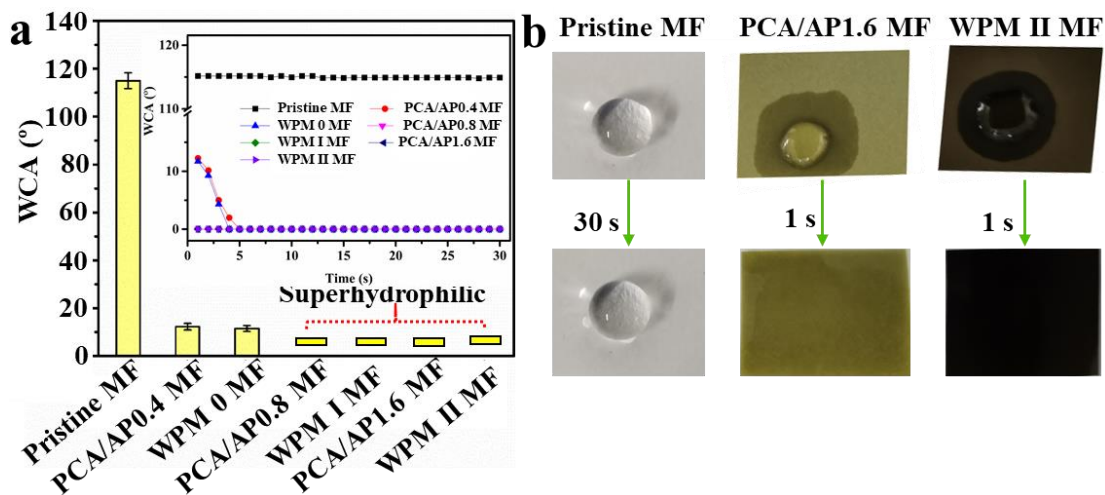
98



99

100 **Supplementary Figure 12|** The C 1s, N 1s and Fe 2p spectrum of WPM II MF².

101

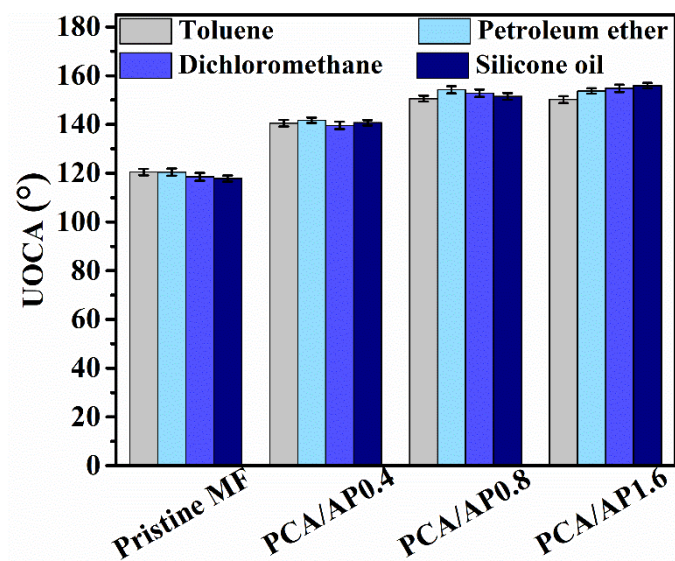


102

103 **Supplementary Figure 13|** (a) and (b) WCA and UOCA of different membranes. Error
 104 bars represent the standard deviations obtained from three membranes

105 Water contact angle (WCA) is comprehensively investigated the surface wettability of
 106 membranes. The pristine MF showed high hydrophobic with the initial WCA of 120 °,
 107 and water (30 μL) remained for 30 seconds without spreading on the surface of this
 108 membrane (see Supplementary Fig. 13). Diversely, thanks to the hydrophilic phenolic
 109 hydroxyl group/amino group, PCA/AP MFs were more affinity to water. PCA/AP0.8,
 110 PCA/AP1.6 MF and all the WPM MFs reached superhydrophilicity. These results
 111 showed the coating microparticles on the membrane surface endowed them with
 112 excellent affinity with water.

113

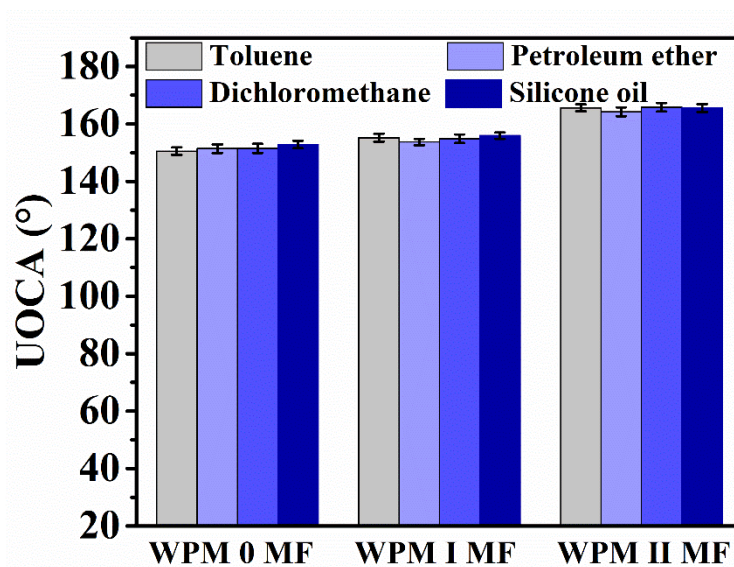


114

115 **Supplementary Figure 14** | The UOCA of PCA/AP MFs. Error bars represent the

116 standard deviations obtained from three membranes

117

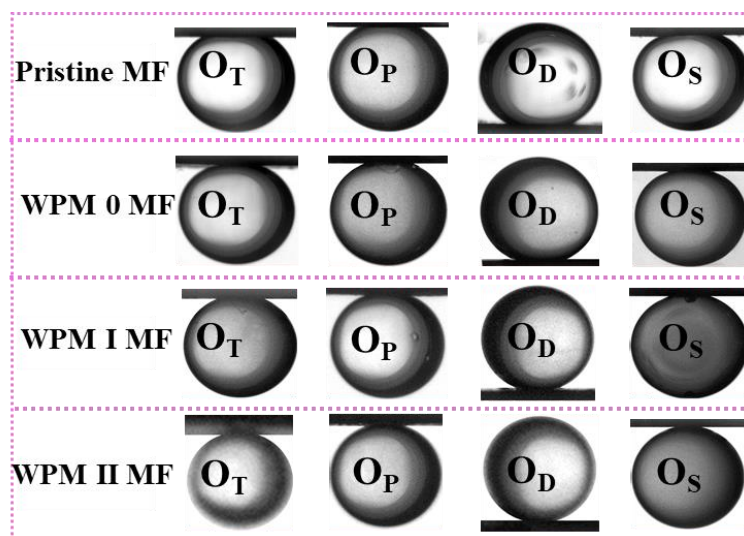


118

119 **Supplementary Figure 15** | The UOCA of WPM MFs. Error bars represent the

120 standard deviations obtained from three membranes

121



122

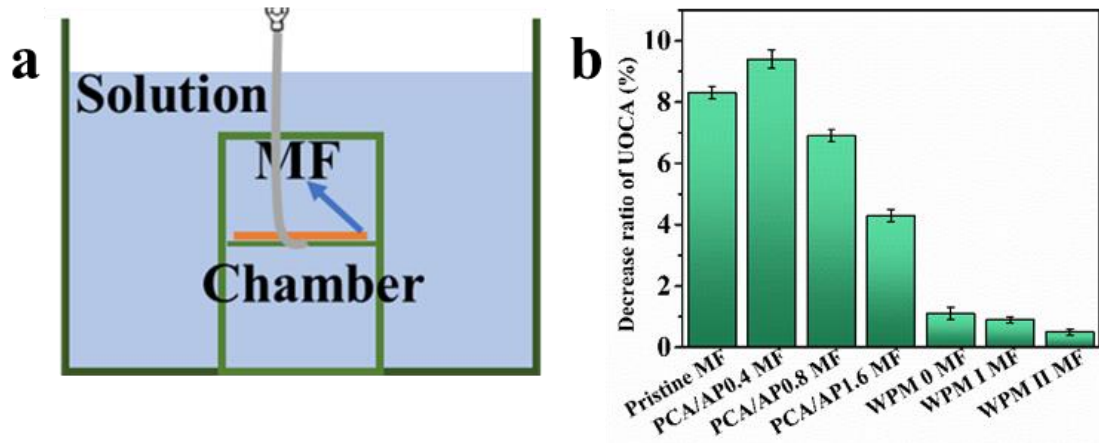
123 **Supplementary Figure 16** Photographs of the underwater oil droplets on the surface
 124 of different membranes (O_T is UOCA of toluene on the membrane surface; O_P is UOCA
 125 of petroleum ether on the membrane surface; O_D is UOCA of dichloromethane on the
 126 membrane surface; O_S is UOCA of silicone oil on the membrane surface).

127 Compared with the original MF, under water oleophobic performance of the
 128 PCA/AP0.4 membrane was enhanced (UOCA were about 140°). Furthermore, both of
 129 PCA/AP0.8 and PCA/AP1.6 MF had underwater oleophobicity with UOCA all greater
 130 than 145° . In addition, after modified by Fe^{3+} , WPM MFs possessed stronger
 131 underwater superoleophobicity properties than that of the corresponding PCA/AP MFs
 132 (see Supplementary Figs. 14-16). The result was mainly attributed to the synergistic
 133 effect of the construction of micro/nano structure and abundant hydrophilic groups.

134

135

136

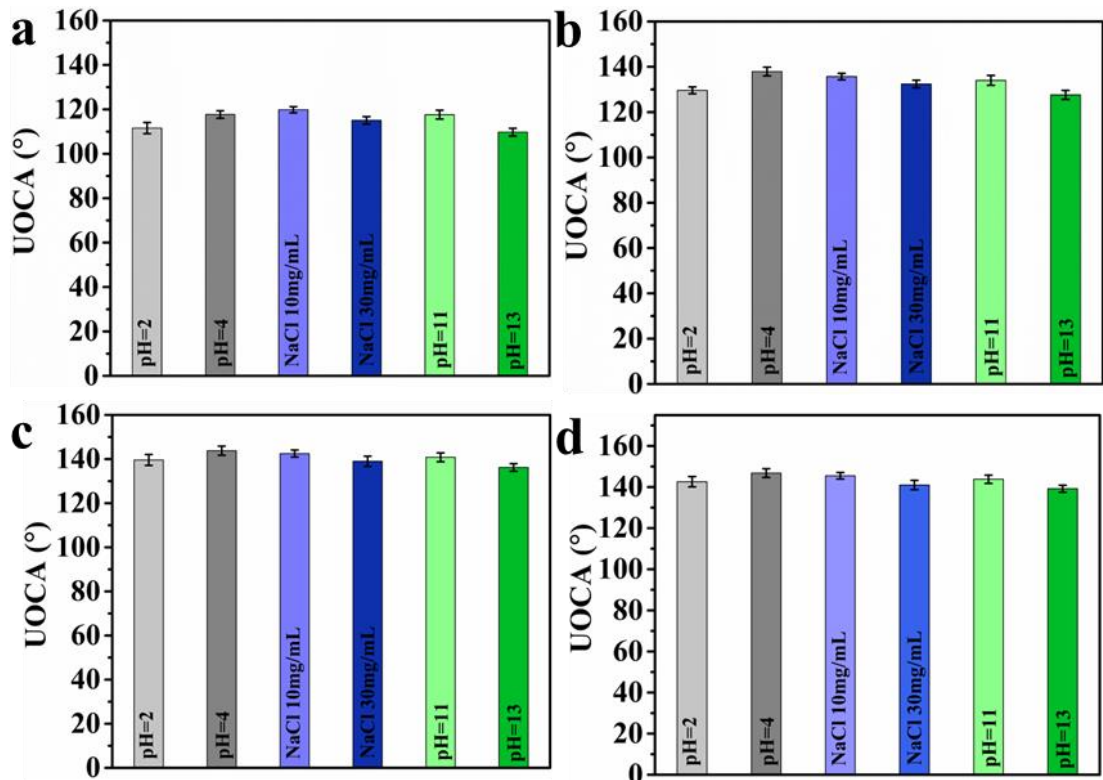


137

138 **Supplementary Figure 17** | (a) Device suitable for testing UOCA and (b) The decrease
 139 ratio of the UOCA values for each membrane after immersed in alkaline aqueous
 140 solution (pH=13) for 24 h. The error bar represents the standard deviation of the
 141 measurements.

142

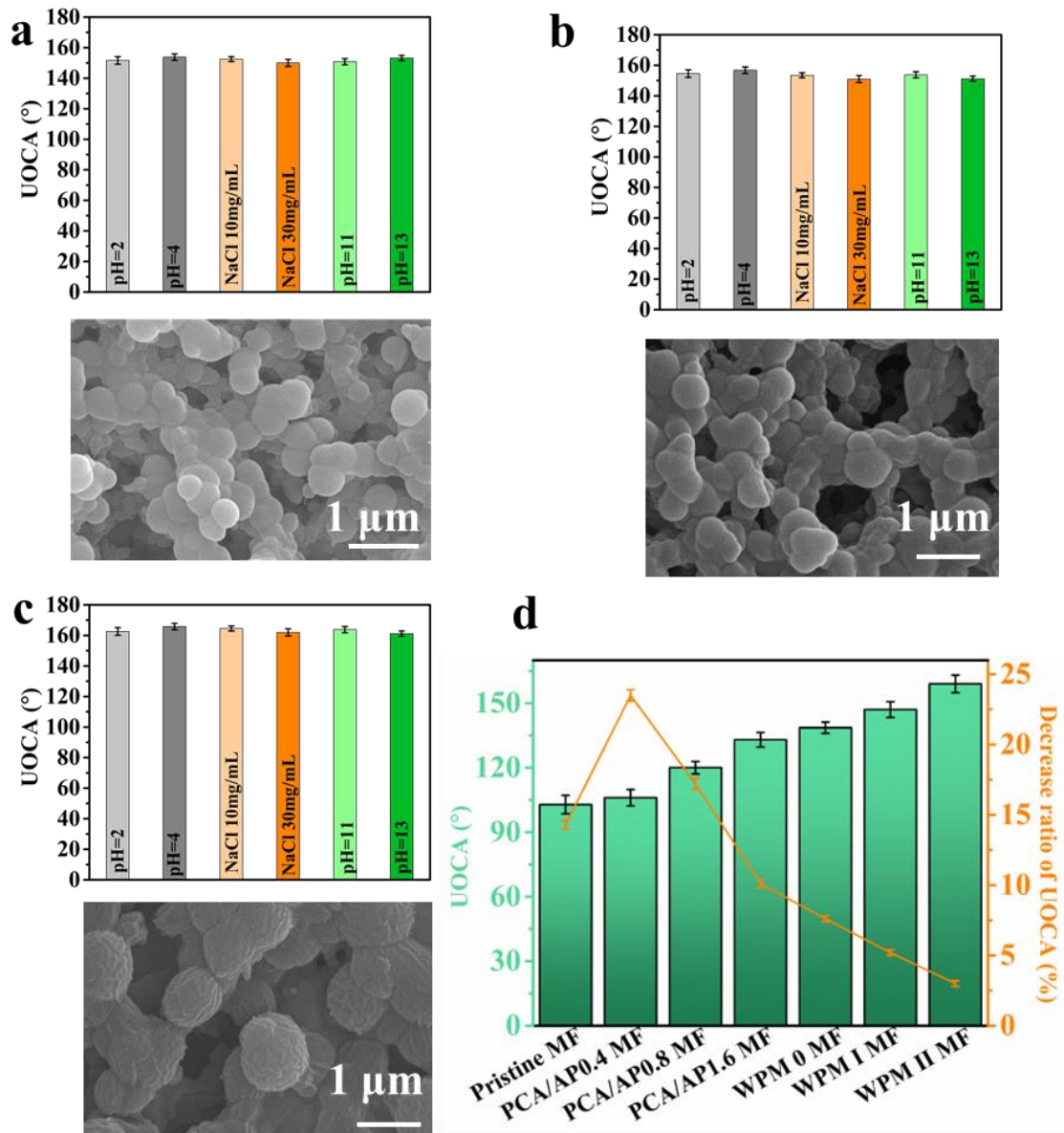
143



144

145 **Supplementary Figure 18** | (a) The pristine MF; (b) PCA/AP0.4; (c) PCA/AP0.8; (d)
 146 PCA/AP1.6. The error bar represents the standard deviation of the measurements.

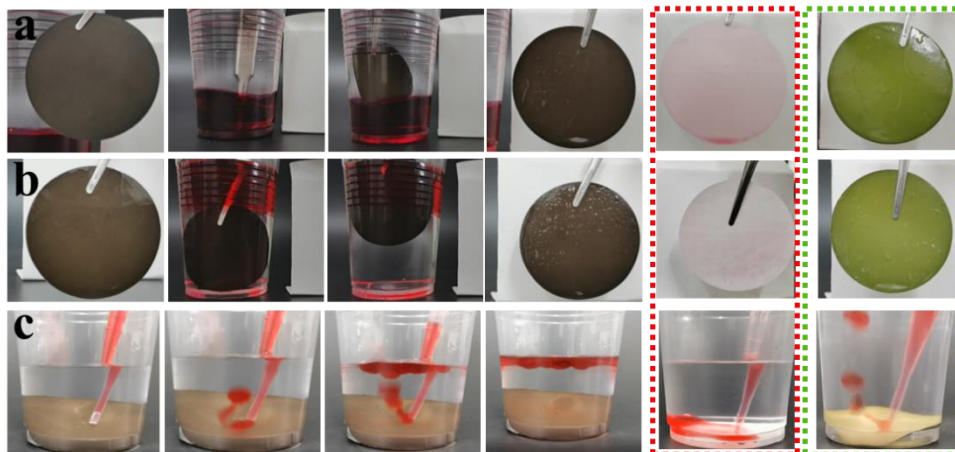
147



148

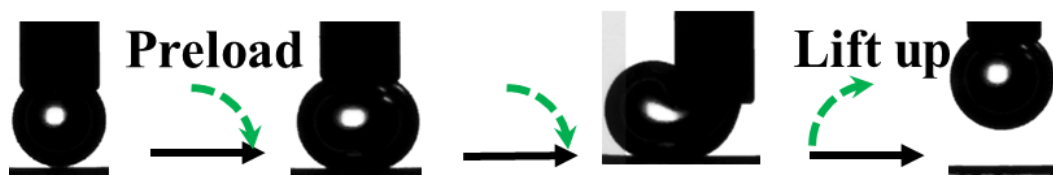
149 **Supplementary Figure 19** | The UOCA of (a) WPM 0; (b) WPM I; (c) WPM II MF
 150 after immersed in acidic, alkaline aqueous solution or saline solution for 24 h. (d)
 151 UOCA and the decrease ratio of the values for each membrane after immersed in acidic
 152 solution for 7 days. The error bar represents the standard deviation of the measurements.
 153 To further investigate the chemical stability of all membranes, we detected the UOCA
 154 of the membranes after immersing it into acidic, alkaline or saline solution for 24 h (see
 155 Supplementary Figs. 17-19). The results show the well chemical stability of WPM MFs,
 156 while UOCAs of PCA/AP membranes showed a downward trend under the acid, base
 157 or saline solution environment. Because of the greater drop of UOCA after immersed
 158 in alkaline aqueous solution (pH=13) for 24 h, we further tested the decrease ratio of

159 the UOCA values for each membrane after immersed in alkaline aqueous solution
 160 (pH=13) for 24 h. The results showed that the decrease ratio of UOCA of PCA/AP MFs
 161 decreased with the increase of APTES content, indicating that the increase of
 162 hydrophilic microparticles coating was conducive to the chemical stability of the
 163 membrane. In addition, we tested the UOCA and the decrease ratio of UOCA of each
 164 membrane after immersed in alkaline aqueous solution (pH=13) for 7 days to give the
 165 more powerful proof of the more stable underwater high oleophobic properties of WPM
 166 MFs. The results indicated that when the soaking time increased, the values of the
 167 original and PCA/AP MFs would decrease more and the decrease ratio was larger,
 168 showing they cannot be used in long-term oil/water separation. While, WPM MFs still
 169 retained high underwater oleophobic properties, especially UOCA of WPM II MF
 170 maintained above 160 ° and possessed stable underwater superoleophobicity property.
 171



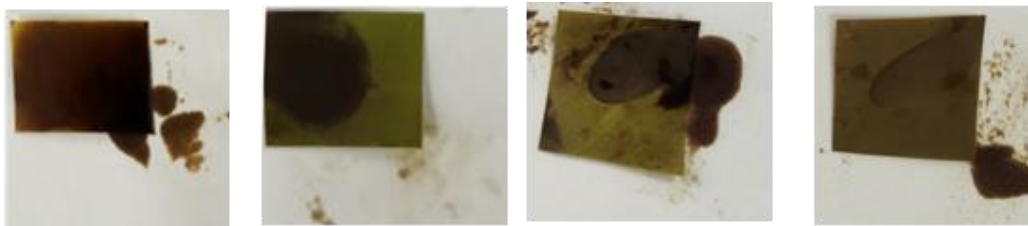
172
 173 **Supplemental Figure 20** | Anti-low viscous oil fouling performance of the pristine,
 174 PCA/AP1.6 and WPM II MF. **(a)** The heavy oil fouling resistance; **(b, c)** The light oil
 175 fouling resistance. All oils are dyed red.

176



177

178 **Supplemental Figure 21** | Underwater oil adhesion process on WPM II MF.



Pristine MF PCA/AP1.6 MF WPM 0 MF WPM I MF

179

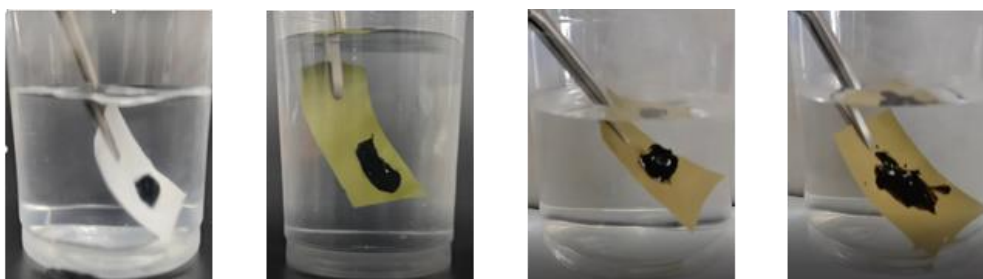
180

Supplemental Figure 22 | Anti- dilute crude oil fouling performance of the

181

membranes.

182



Pristine MF PCA/AP1.6 MF WPM 0 MF WPM I MF

183

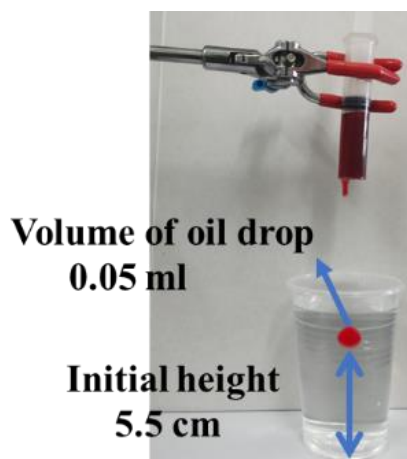
184

Supplemental Figure 23 | Anti- dilute crude oil fouling performance of the

185

membranes.

186

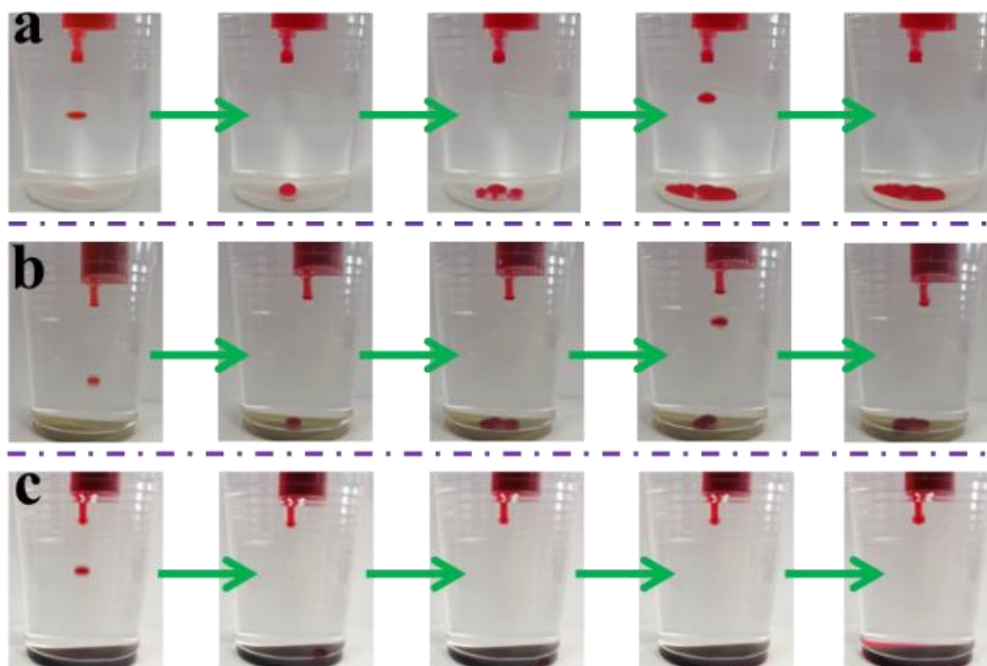


187

188

Supplemental Figure 24 | Schematic of Free-falling experiment.

189

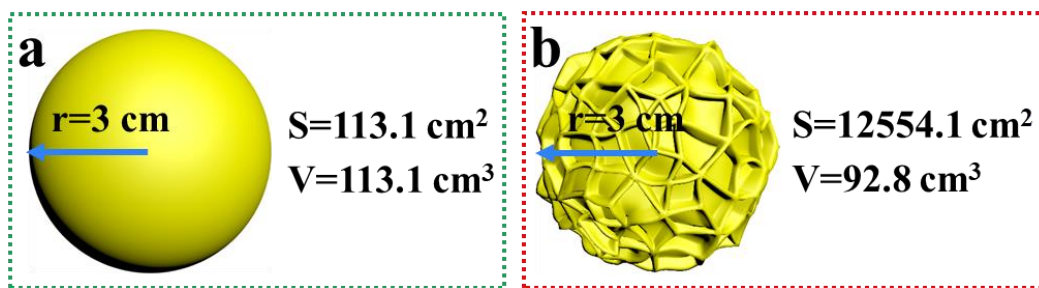


190

191 **Supplemental Figure 25**| Free-falling experiment of oil droplets in water on **(a)** The
 192 pristine; **(b)** WPM 0; **(c)** WPM II MF.

193 We tested the free-falling experiment for each membrane. After oil droplet fell on the
 194 surface of the pristine MF, it firmly adhered to the placement, and not fell off even if
 195 shaken violently. The oil droplets rolled from the falling point to other positions of the
 196 surface of PCA/AP MFs, WPM 0 MF and WPM I MF finally stop at a certain position
 197 on the membrane surface. However, oil drops immediately bounced up like a ball after
 198 touched WPM II MF surface, then slipped into the water after touching the membrane
 199 surface again. The results illustrated different from other non-migratory foulant, oil
 200 fouling not only contaminated the impact point, but migrated or amalgamated at other
 201 positions on the membrane surface, thus improving the resistance to oil fouling was
 202 more challenging. Also, the different trajectories of oil droplets contacting the surfaces
 203 of WPM 0 and WPM II MF indicated that their anti-oil-fouling mechanisms were
 204 different.

205



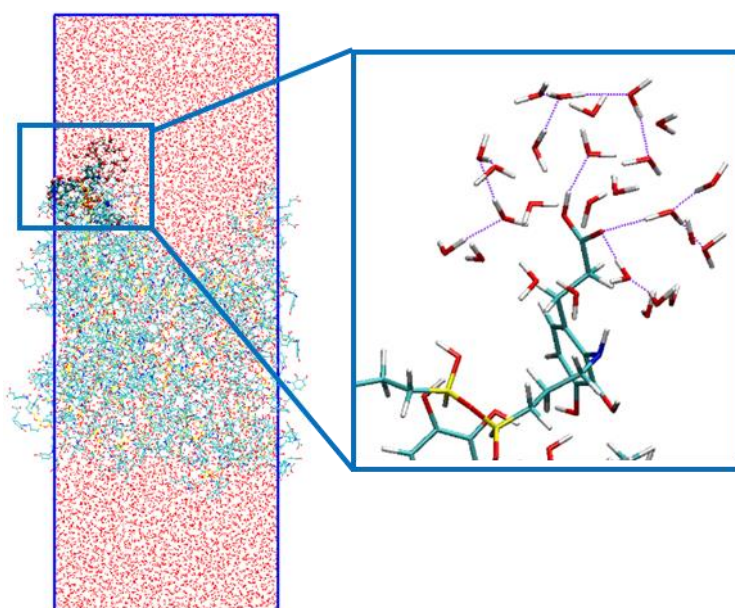
206

207 **Supplemental Figure 26** | The surface area and volume of the smooth microparticles

208 (a, PCA/AP1.6) and the corresponding microparticles with wrinkled patterns (b,

209 WPM II) were calculated by simulation.

210

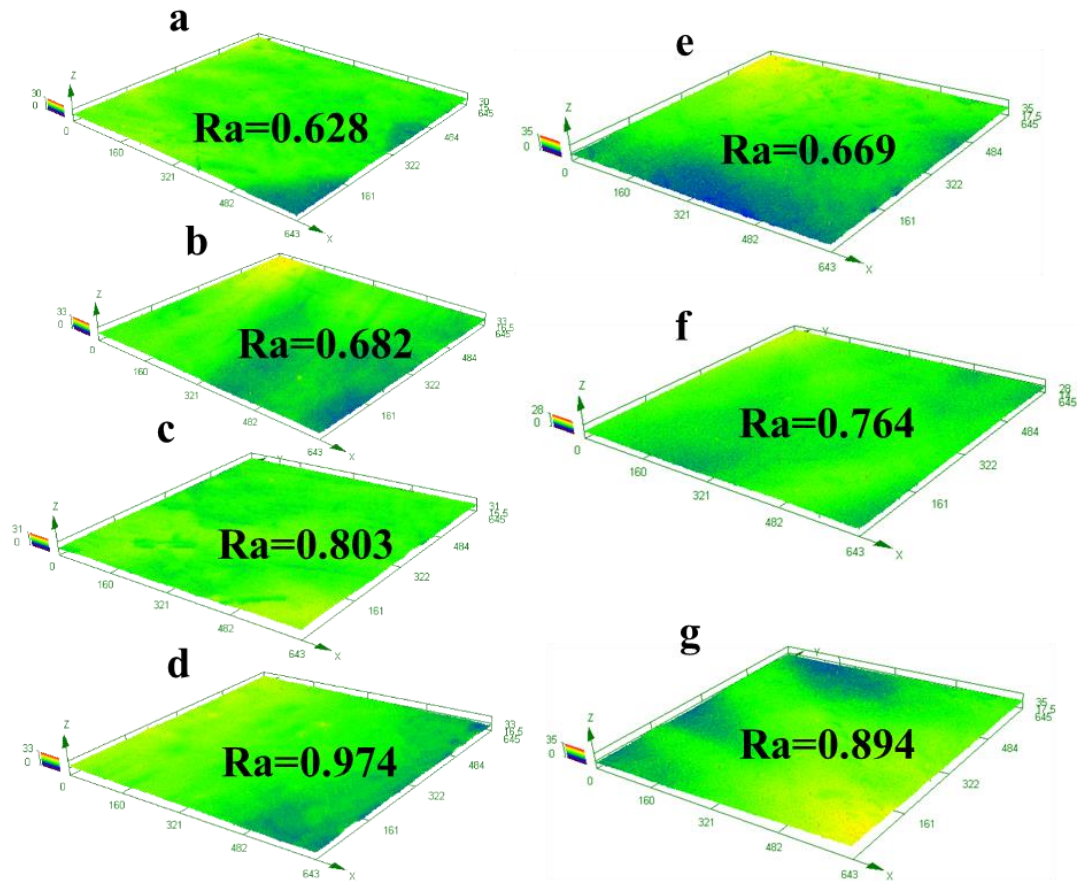


211

212 **Supplemental Figure 27** | Structure of PCA/AP1.6 MF/water molecular with enhanced

213 hydrogen bonds formed between membranes and hydration layer water.

214

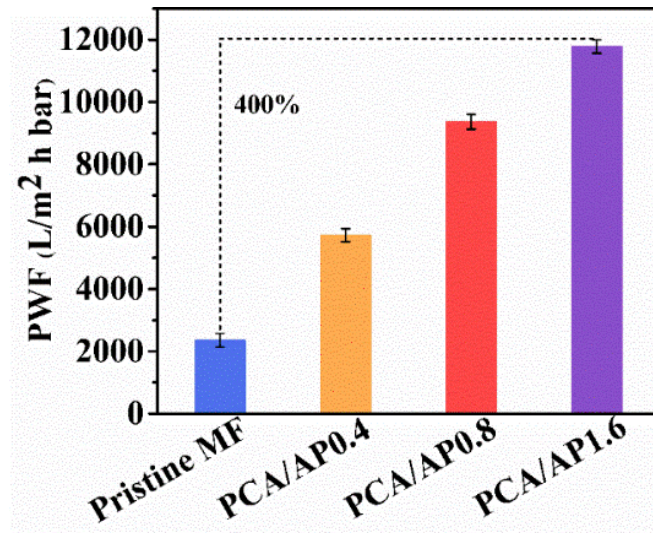


215

216 **Supplementary Figure 28** | CLSM images of (a) the pristine; (b) PCA/AP0.4; (c)
 217 PCA/AP0.8; (d) PCA/AP1.6; (e) WPM 0; (f) WPM I; (g) WPM II MF.

218 The surface roughness of the WPM 0 MF ($R_a=0.669 \mu\text{m}$) increased by 6.6% compared
 219 to that of the pristine MF ($R_a=0.628 \mu\text{m}$) and decreased by 1.9% compared to that of
 220 the PCA/AP0.4 MF ($R_a=0.682 \mu\text{m}$). The surface roughness of WPM I MF ($R_a=0.764$
 221 μm) increased 25% than that of the pristine MF and decreased 4.9% than that of
 222 PCA/AP0.8 MF ($R_a=0.803 \mu\text{m}$), respectively. Besides, the roughness of WPM II MF
 223 ($R_a=0.894 \mu\text{m}$) was 8.2% lower than that of PCA/AP1.6 MF ($R_a=0.974 \mu\text{m}$) and 42%
 224 higher than that of the pristine MF. The largest size of PCA/AP1.6 microparticles
 225 caused the average distance between the contour peak line and the membrane surface
 226 became higher after coating on the membrane surface, resulting in the maximum
 227 roughness. While, the wrinkling formed by WPM microparticles would reduce the
 228 average distance between the microparticles surface contour and the membrane surface
 229 and then the roughness of WPM MFs declined.

230

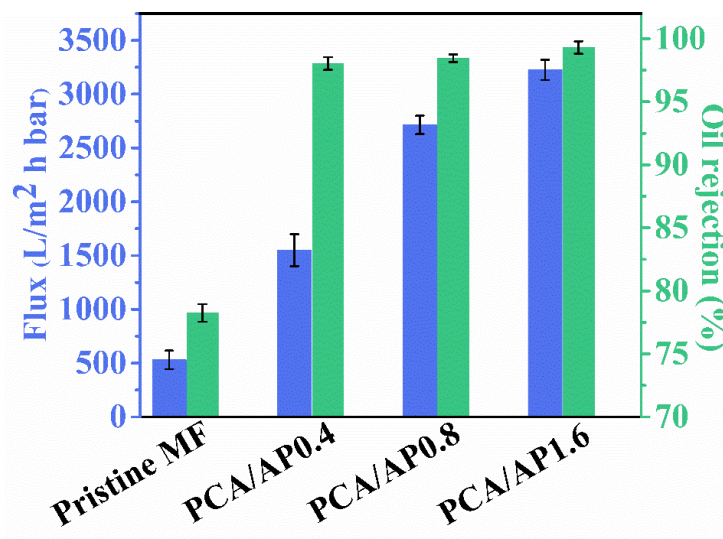


231

232 **Supplementary Figure 29** | The pure water flux of different membranes.

233 The PWF of WPM I MF reached 12522 L m⁻² h⁻¹ bar, a 510% and 350% improvement
 234 when compared to commercial pristine and PCA/AP0.8 MF. The PWF of WPM 0 MF
 235 reached 7800 L m⁻² h⁻¹ bar, a 290% and 270% improvement when compared to
 236 commercial pristine and PCA/AP0.4 MF (see Supplementary Fig. 29).

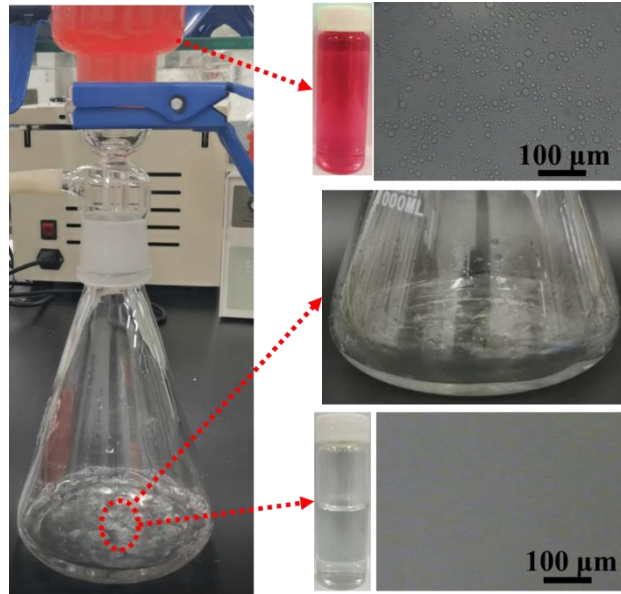
237



238

239 **Supplementary Figure 30** | The filtration flux and oil rejection of different membranes.

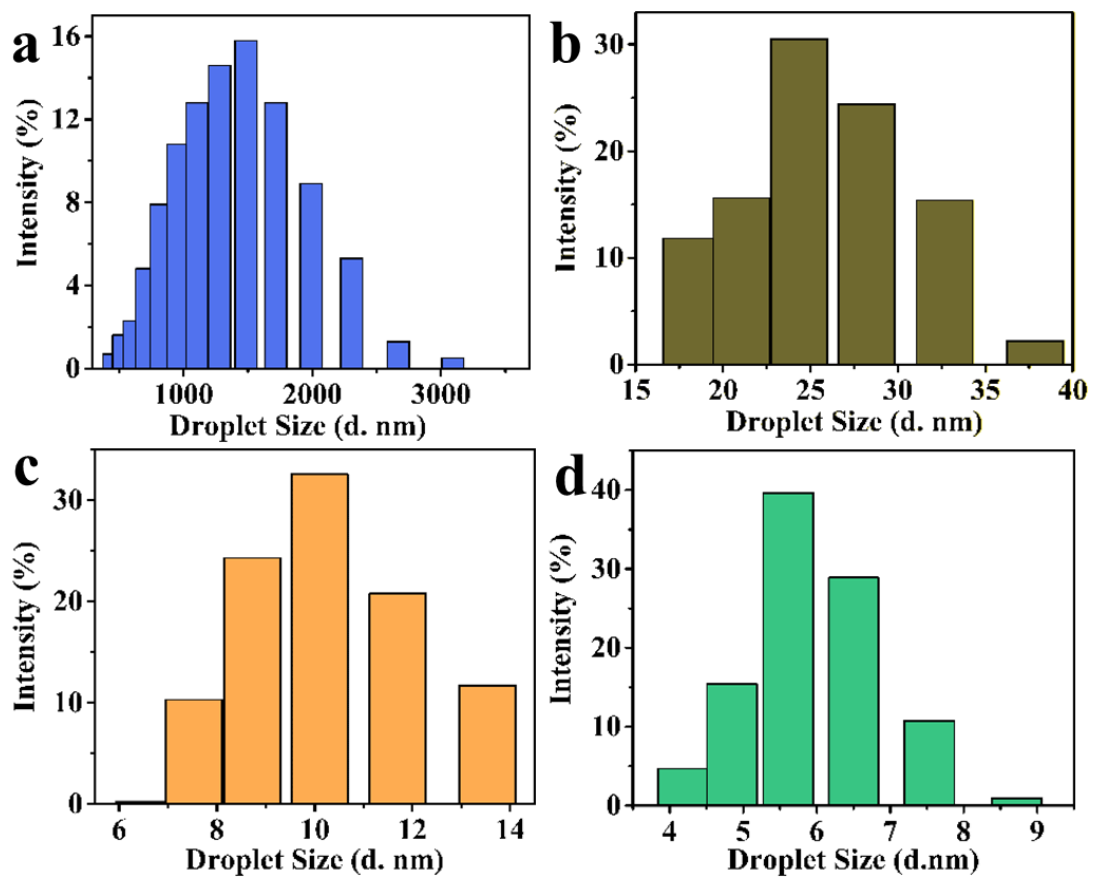
240



241

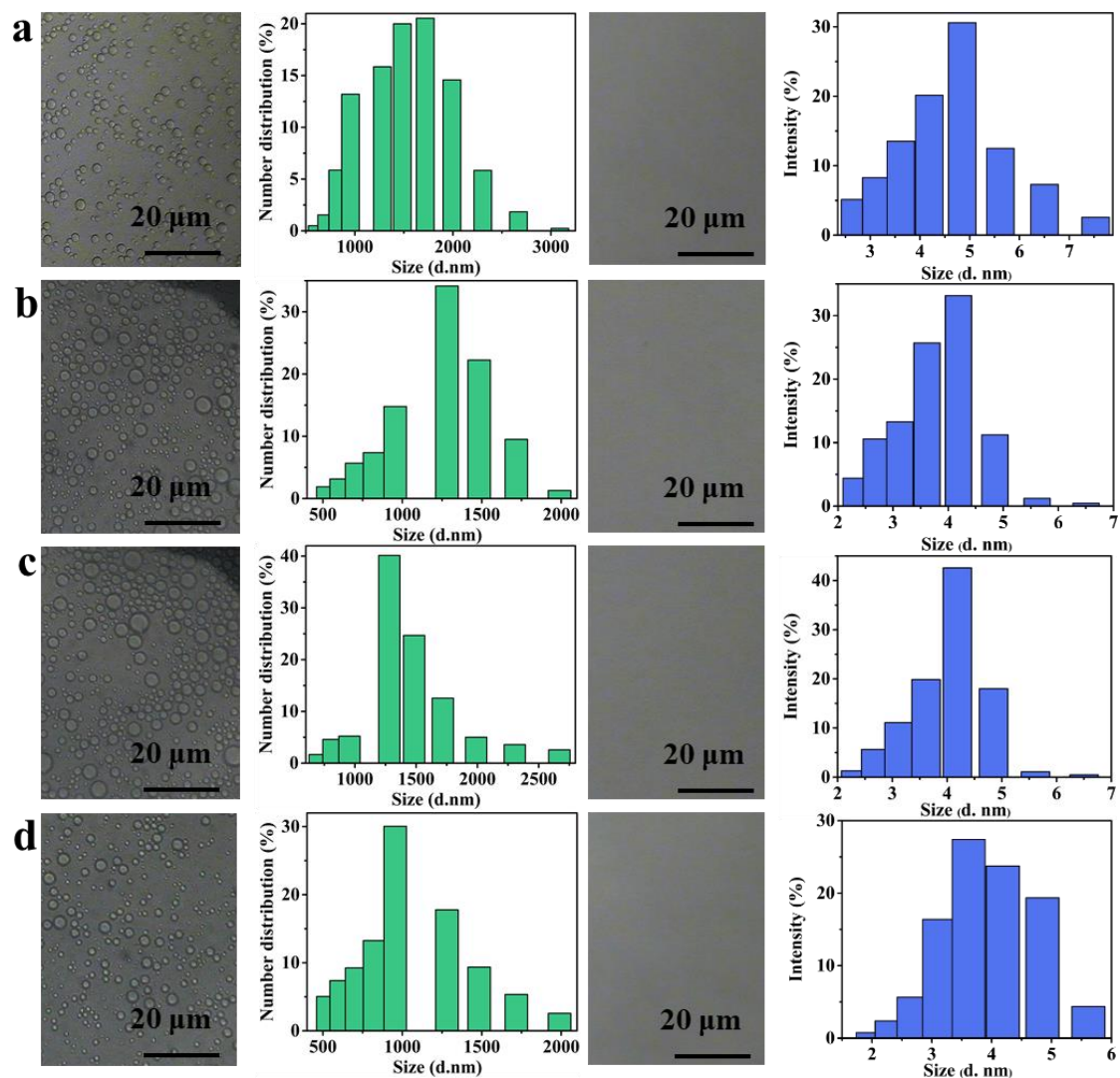
242 **Supplementary Figure 31** | The photographs of filtration process and optical
 243 microscope images of T/W emulsion before and after filtration

244



245

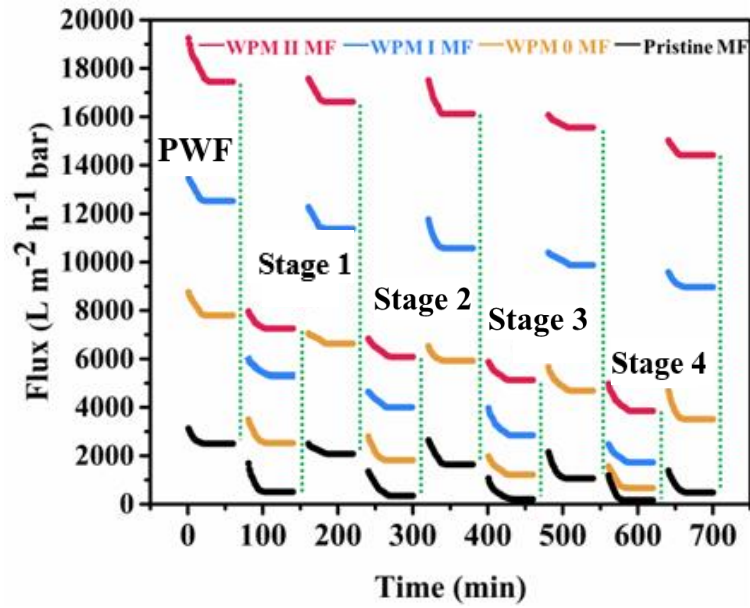
246 **Supplementary Figure 32** | (a) The oil drops in the feed of T/W emulsion before
 247 separation; (b-d) The oil drops in the filtration after T/W emulsion separation of WPM
 248 0, WPM I, WPM II MF.



250

251 **Supplementary Figure 33** | The microscopic images and the oil drops in the feed/
 252 filtration of /W emulsion of WPM II MF. (a) D/W; (b) P/W; (c) Si/W; (d) H/W.

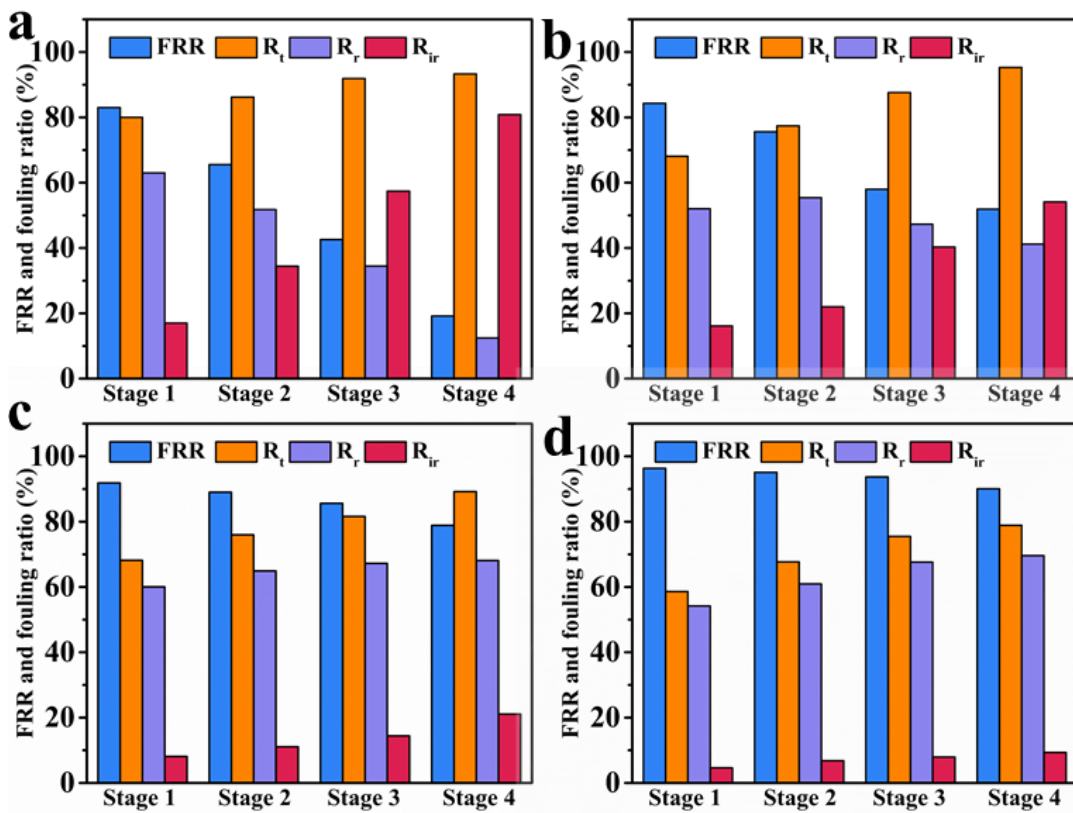
253 The O/W emulsion before filtration was deep pink with a particle size of about 1500
 254 nm, by contrast, the filtrate was almost transparent with no droplets, which was further
 255 confirmed by optical microscopy (see Supplementary Figs. 31-33). After WPM 0 and
 256 WPM I membrane filtration, more than 10 nm oil droplets still penetrated the membrane,
 257 but no 10 nm oil droplets permeated across the WPM II MF, indicating that the WPM
 258 II MF had the optimal O/W separation performance. Then we tested the separation
 259 performance of WPM II MF for different O/W emulsions, and it can be seen that the
 260 particle size of the emulsion in the filtrate filtered by the membrane can reach less than
 261 5 nm.



263

264 **Supplementary Figure 34** | The separation performance of membranes during four-
 265 cycles emulsion separation.

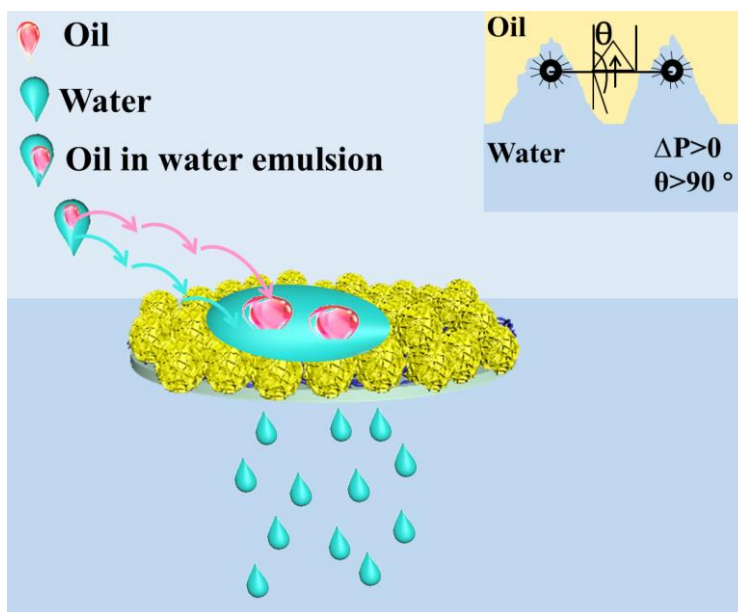
266



267

268 **Supplementary Figure 35** | FRR, R_t, R_r, R_{ir} values of (a) Pristine; (b)
 269 WPM I; (d) WPM II MF during four-cycles emulsion separation.

270

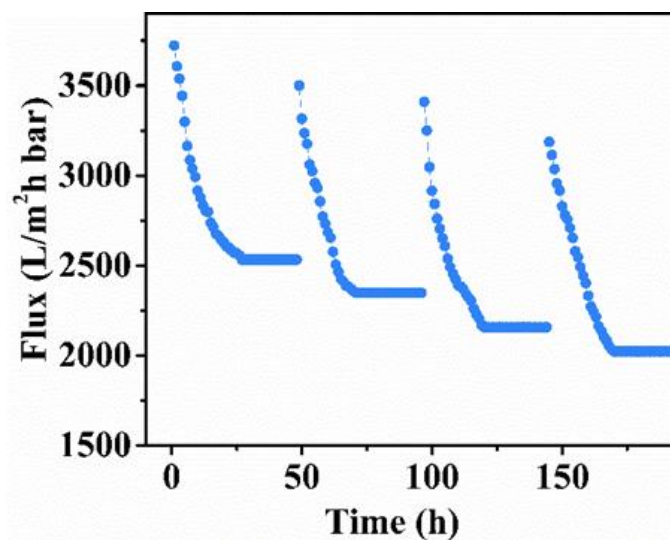


271

272 **Supplementary Figure 36**| Schematic of demulsification mechanism of WPM II MF

273 for crude-oil/water separation.

274

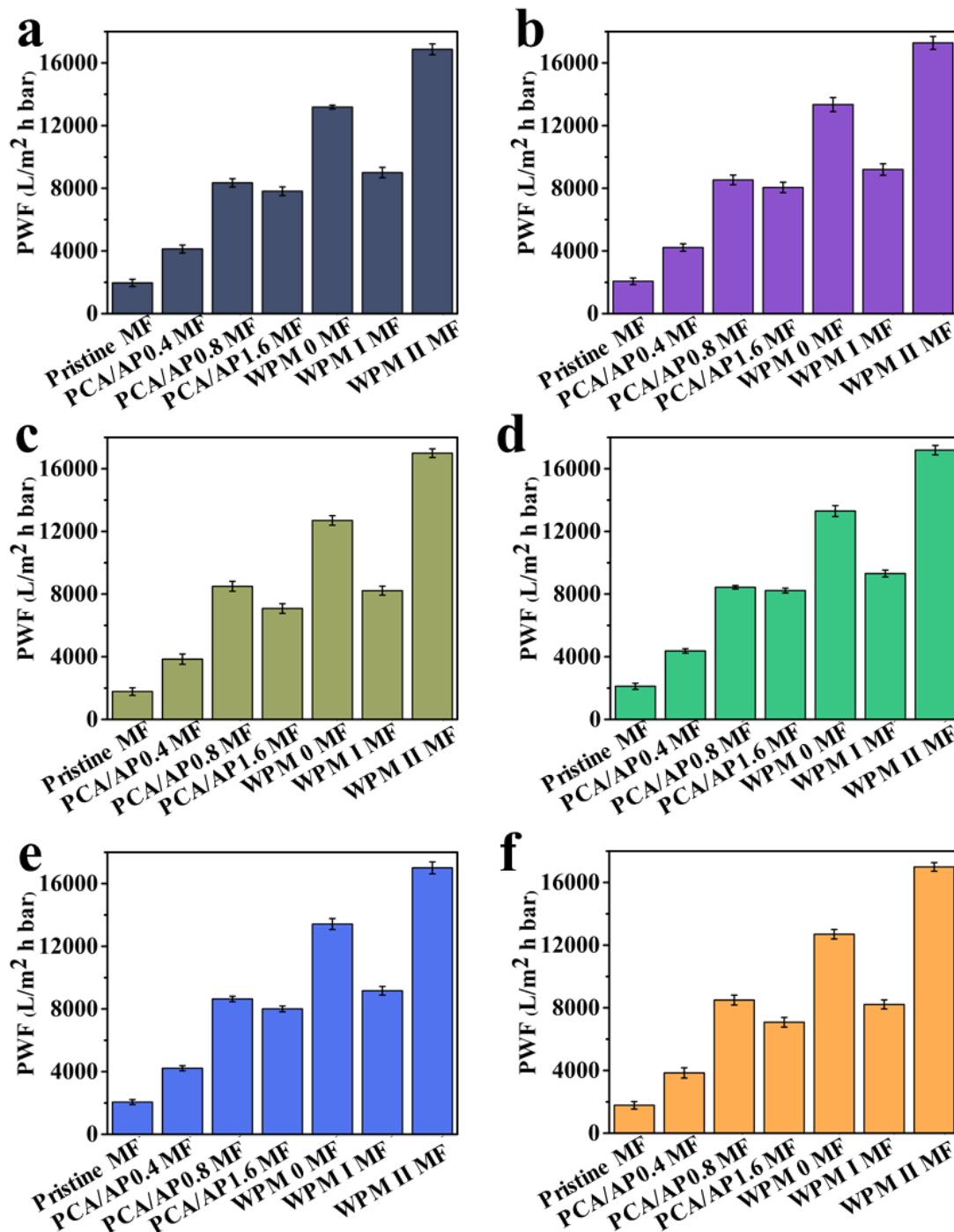


275

276 **Supplementary Figure 37**| Separation performance of viscous crude oil/water

277 mixture of WPM II MF under 1 bar.

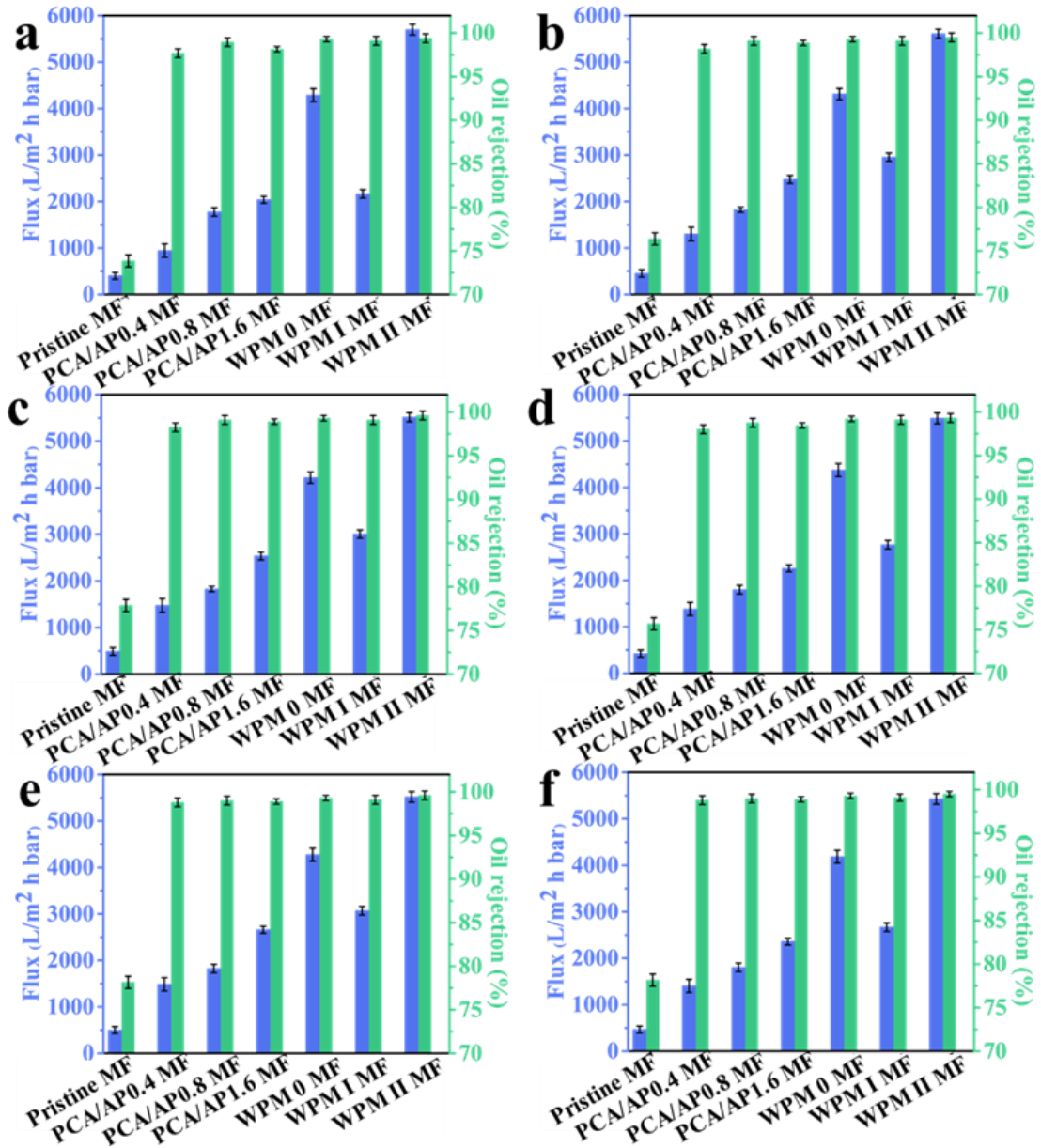
278



279

280 **Supplementary Figure 38** | The pure water flux of different membranes after immersed
 281 in acidic, alkaline aqueous solution or saline solution for 24 h. (a) pH=2; (b) pH=4; (c)
 282 NaCl 10 mg/ml; (d) NaCl 30 mg/ml; (e) pH=11; (f) pH=13.

283

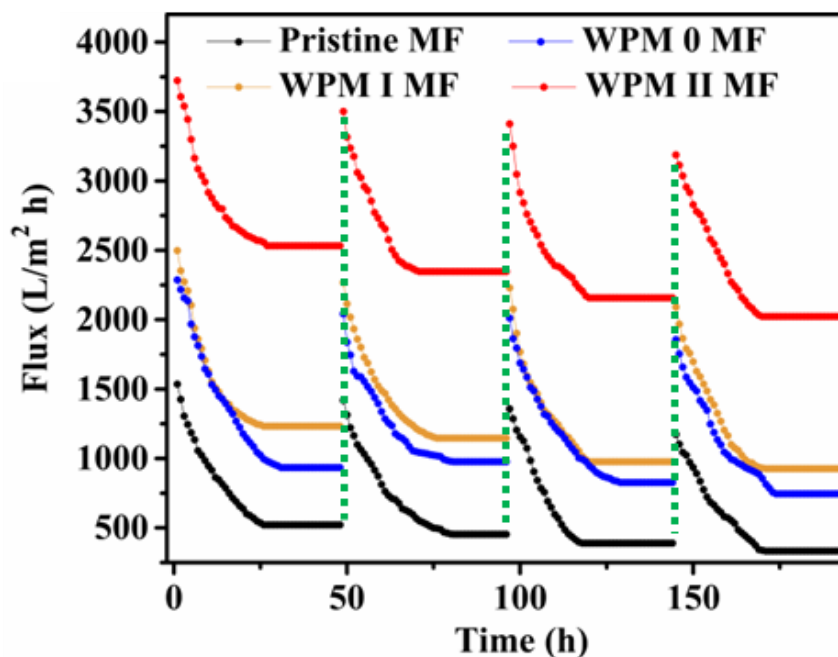


284

285 **Supplementary Figure 39** | The filtration flux and oil rejection of different membranes
 286 after immersed in acidic, alkaline aqueous solution or saline solution for 24 h. **(a)** pH=2;
 287 **(b)** pH=4; **(c)** NaCl 10 mg/ml; **(d)** NaCl 30 mg/ml; **(e)** pH=11; **(f)** pH=13.

288 Afterwards, we examined the stability of the pure water flux and the separation
 289 performance of all the membranes under the acid, base or saline solution environment,
 290 and the results illustrated that the separation performance of membranes modified by
 291 only APTES decreased sharply, and membranes after introduction Fe ions still had high
 292 flux and precise separation performance in acid, base or salt environments.

293

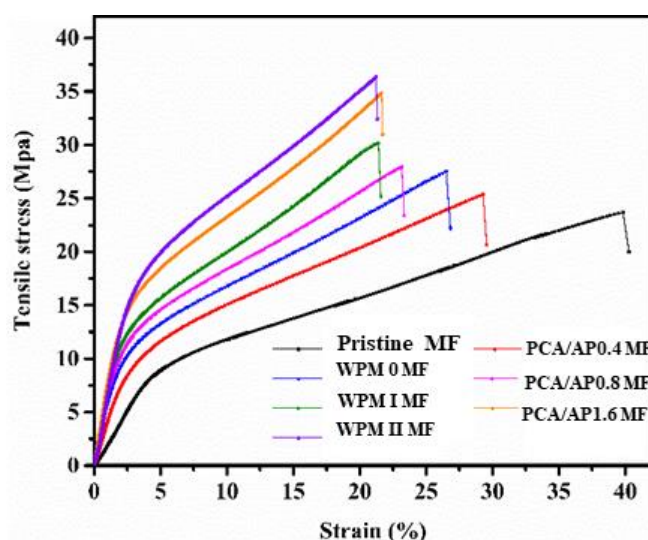


294

295 **Supplementary Figure 40**| Long-term water flux of WPM II MF.

296 Maintaining the long-term separation performance of the membrane is a key factor in
 297 determining its practical application. Thus, we tested the flux of WPM II MF to evaluate
 298 long-term operation stability within 190 h for C/W emulsion separation under 1 bar of
 299 cross-flow filtration. The flux of WPM II MF in Supplementary Fig. 40 showed the
 300 separation flux still maintained above 2000 L m⁻² h⁻¹ bar after 190 hours of operation,
 301 which had a well long-term operation stability under cross-flow filtration mode,
 302 illustrating WPM II MF has potential application in oily wastewater treatment.

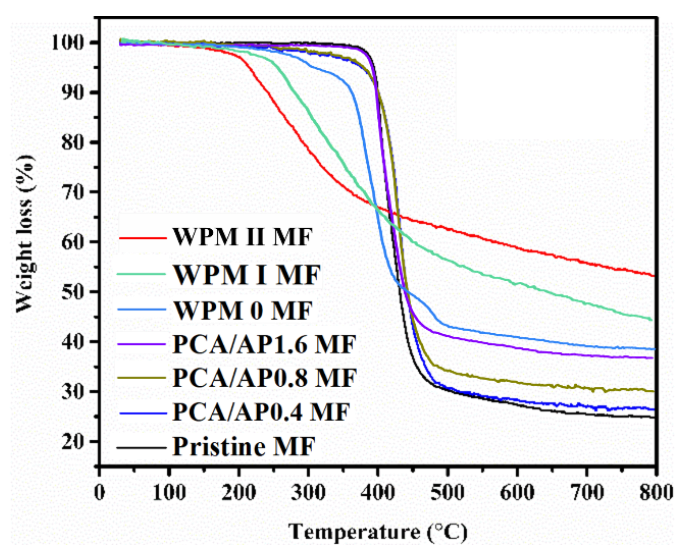
303



304

305 **Supplementary Figure 41**| Mechanical properties using tensile tests of membranes.

306



307

308 **Supplementary Figure 42**| TGA of membranes.

309 **Supplementary Table 1**| The detailed modification conditions and abbreviations of the
 310 membranes.

| Membranes | CA (g) | APTES (g) | FeCl ₃ (mg/ml) | Reaction Time (h) | Temperature (°C) |
|--------------|--------|--------------|------------------------------|----------------------|---------------------|
| Pristine MF | 0 | 0 | 0 | 12 | 25 |
| PCA/AP0.4 MF | 0.2 | 0.4 | 0 | 12 | 25 |
| WPM 0 MF | 0.2 | 0.4 | 100 | 12 | 25 |
| PCA/AP0.8 MF | 0.2 | 0.8 | 0 | 12 | 25 |
| WPM I MF | 0.2 | 0.8 | 100 | 12 | 25 |
| PCA/AP1.6 MF | 0.2 | 1.6 | 0 | 12 | 25 |
| WPM II MF | 0.2 | 1.6 | 100 | 12 | 25 |

311

312 **Supplementary Table 2**| Summary of the DFT simulation results.

| System | Binding energy (kJ/mol) | E _{complex} (kJ/mol) | E _{fragment1} (kJ/mol) | E _{fragment2} (kJ/mol) |
|----------------------|-------------------------------|----------------------------------|------------------------------------|------------------------------------|
| Fe ³⁺ -OH | -151.79 | -3049.642 | -1786.377 | -1263.208 |

| | | | | |
|------------------------|---------|-----------|-----------|-----------|
| Fe ³⁺ -NH | -221.93 | -3049.663 | -1786.371 | -1263.208 |
| Fe ³⁺ -COOH | -217.48 | -3049.666 | -1786.375 | -1263.208 |

313

314 **Supplementary Table 3** | Surface elemental analysis of the membranes from the XPS
315 spectra.

| Samples | Elemental and Area/% | | | | | |
|--------------|----------------------|-------------|-------------|-------------|--------------|---------------|
| | C <i>1s</i> | N <i>1s</i> | F <i>1s</i> | O <i>1s</i> | Si <i>2p</i> | Fe <i>2p3</i> |
| Pristine MF | 59.11 | 1.77 | 34.72 | 4.05 | 0.35 | 0 |
| PCA/AP0.4 MF | 60.58 | 5.28 | 1.39 | 23.06 | 9.7 | 0 |
| WPM 0 MF | 63.19 | 4.4 | 2.18 | 22.4 | 7.42 | 0.41 |
| PCA/AP0.8 MF | 57.78 | 6.91 | 1.53 | 22.75 | 11.02 | 0 |
| WPM IMF | 59.23 | 4.29 | 2.17 | 25.55 | 6.18 | 2.58 |
| PCA/AP1.6 MF | 57.23 | 6.85 | 2.94 | 21.34 | 11.65 | 0 |
| WPM IIMF | 55.24 | 3.74 | 1.23 | 30.38 | 5.64 | 3.78 |

316

317 **Supplementary Table 4** | XPS results of all membranes.

| Samples | Elemental and Atomic /% | POS. | Peak attribution | Area/% | Molar fraction/% |
|-----------------|----------------------------------|--------|---------------------|--------|---------------------|
| Pristine MF | C <i>1s</i> | 283.54 | C-C | 51.98 | 30.73 |
| | (59.11) | 285.46 | C-O | 45.11 | 26.66 |
| | | 291.08 | C-F | 2.91 | 1.72 |
| Pristine MF | O <i>1s</i> | 530.27 | C-O | 100 | 4.05 |
| | (4.05) | | | | |
| Pristine MF | N <i>1s</i> | 400.81 | N-H | 100 | 1.77 |
| | (1.77) | | | | |
| PCA/AP0.4 MF | C <i>1s</i> | 284.60 | C-C/C=C | 17.12 | 10.37 |
| | (60.58) | 287.88 | C-O | 14.91 | 9.03 |

| | | | | | |
|-----------|-------------------|--------|---------|-------|-------|
| | | 290.84 | C-F | 12.02 | 7.28 |
| | | 283.86 | C-Si | 15.39 | 9.32 |
| | | 287.88 | C=O | 13.58 | 8.23 |
| | | 286.24 | C=N | 13.86 | 8.40 |
| | | 285.76 | C-N | 13.13 | 7.95 |
| | O <i>1s</i> | 533.48 | -OH | 58.04 | 13.38 |
| | (23.06) | 530.67 | -O-C | 25.42 | 5.86 |
| | | 529.38 | O=C | 16.54 | 3.81 |
| | N <i>1s</i> | 401.32 | N-H | 55.88 | 2.95 |
| | (5.28) | 399.38 | N=C | 44.12 | 2.33 |
| WPM 0 | C <i>1s</i> | 291.07 | C-F | 0.12 | 0.08 |
| MF | (63.19) | 287.85 | C=O | 6.55 | 4.14 |
| | | 286.21 | C=N | 22.44 | 14.18 |
| | | 285.35 | C-N | 22.32 | 14.11 |
| | | 284.81 | C-O | 17.93 | 11.33 |
| | | 284.31 | C=C/C-C | 22.28 | 14.08 |
| | | 283.84 | C-Si | 8.35 | 5.28 |
| | O <i>1s</i> | 533.36 | -O-C | 13.12 | 2.94 |
| | (22.4) | 532.69 | O=C | 34.80 | 7.8 |
| | | 531.97 | -OH | 17.16 | 3.84 |
| | | 531.06 | O-Fe | 34.92 | 7.82 |
| | N <i>1s</i> (4.4) | 401.61 | N-H | 50.25 | 2.21 |
| | | 399.50 | N=C | 39.74 | 1.75 |
| | | 395.61 | N-Fe | 10.01 | 0.44 |
| PCA/AP0.8 | C <i>1s</i> | 291.36 | C-F | 2.33 | 1.35 |
| MF | (57.78) | 287.76 | C=O | 8.08 | 4.67 |
| | | 286.10 | C=N | 14.07 | 8.13 |
| | | 285.26 | C-N | 10.47 | 6.05 |

| | | | | | |
|-----------|-------------|--------|---------|-------|-------|
| | | 284.83 | C-O | 17.95 | 10.37 |
| | | 284.22 | C C/C=C | 19.66 | 11.36 |
| | | 283.76 | C-Si | 27.44 | 15.85 |
| | O <i>1s</i> | 532.72 | -O-C | 16.84 | 3.83 |
| | (22.75) | 531.93 | O=C | 41.02 | 9.33 |
| | | 531.11 | -OH | 42.15 | 9.59 |
| | N <i>1s</i> | 401.32 | N-H | 46.45 | 3.21 |
| | (6.91) | 399.38 | N=C | 53.55 | 3.70 |
| WPM I MF | C <i>1s</i> | 291.07 | C-F | 0.12 | 0.08 |
| | (59.23) | 287.85 | C=O | 6.55 | 4.14 |
| | | 286.21 | C=N | 22.44 | 14.18 |
| | | 285.35 | C-N | 22.32 | 14.11 |
| | | 284.81 | C-O | 17.93 | 11.33 |
| | | 284.31 | C=C/C-C | 22.28 | 14.08 |
| | | 283.84 | C-Si | 8.35 | 5.28 |
| | O <i>1s</i> | 529.70 | O-Fe | 22.95 | 5.86 |
| | (25.55) | 530.97 | -OH | 36.66 | 9.37 |
| | | 531.99 | O=C | 26.34 | 6.73 |
| | | 533.05 | -O-C | 14.04 | 3.59 |
| | N <i>1s</i> | 401.22 | N-H | 48.63 | 2.08 |
| | (4.29) | 399.00 | N=C | 34.20 | 1.47 |
| | | 399.86 | N-Fe | 17.18 | 0.74 |
| PCA/AP1.6 | C <i>1s</i> | 290.85 | C-F | 4.80 | 2.74 |
| | (57.23) | 287.96 | C=O | 11.24 | 6.43 |
| | | 286.46 | C=N | 17.60 | 10.07 |
| | | 285.66 | C-N | 18.18 | 10.41 |
| | | 285.00 | C-O | 20.73 | 11.86 |
| | | 284.50 | C=C/C-C | 24.07 | 13.78 |
| | | 284.02 | C-Si | 3.38 | 1.93 |

| | | | | | |
|--------|-------------|--------|---------|-------|-------|
| | O <i>Is</i> | 532.59 | -O-C | 24.33 | 5.19 |
| | (21.34) | 531.93 | O=C | 58.30 | 12.44 |
| | | 530.74 | -OH | 17.37 | 3.71 |
| | N <i>Is</i> | 400.95 | N-H | 38.77 | 2.66 |
| | (6.85) | 399.12 | N=C | 61.23 | 4.19 |
| WPM II | C <i>Is</i> | 291.08 | C-F | 0.13 | 0.07 |
| MF | (55.24) | 287.73 | C=O | 5.91 | 3.26 |
| | | 286.14 | C=N | 22.13 | 12.22 |
| | | 285.25 | C-N | 22.01 | 12.16 |
| | | 284.71 | C-O | 18.39 | 10.16 |
| | | 284.23 | C=C/C-C | 22.86 | 12.63 |
| | | 283.79 | C-Si | 8.57 | 4.73 |
| | O <i>Is</i> | 529.33 | O-Fe | 18.24 | 5.54 |
| | (30.38) | 530.61 | -OH | 33.81 | 10.27 |
| | | 531.71 | O=C | 31.39 | 9.54 |
| | | 533.23 | -O-C | 16.55 | 5.03 |
| | N <i>Is</i> | 401.21 | N-H | 33.47 | 1.25 |
| | (3.74) | 398.52 | N=C | 34.86 | 1.30 |
| | | 399.58 | N-Fe | 31.67 | 1.19 |

318

319 **Supplementary Table 5** | The viscosity of various liquids.

| Samples | Viscosity (mPa·s) | Temperature (°C) |
|-------------------|-------------------|------------------|
| Petroleum ether | 0.3 | 20 |
| Dichloroethane | 0.8 | 20 |
| Dilute crude oil | 44 | 20 |
| Viscous crude oil | 9630 | 20 |

320

321 **Supplementary Table 6**]. Summary of the MD simulation of PCA/AP1.6 and WPM
 322 II MF, including binding and dissociation energies, diffusion coefficients of hydration
 323 layer water.

| System | ΔE^+ (kJ/mol) | ΔE^- (kJ/mol) | Diffusion coefficients (m^2/s) | Residence Time (ps) |
|--------------|--------------------------|--------------------------|--|------------------------|
| PCA/AP1.6 MF | 0.4 | 2.04 | 3.84±0.07 | 4.5 |
| WPM II MF | 0.5 | 3.0 | 1.95±0.17 | 8.22 |

324

325 **Supplementary Table 7**] Polar and disperse components of the liquids.

| Liquids | Surface-energy components (mN/m) | | |
|-----------------|----------------------------------|--------------|--------------|
| | γ_l | γ_l^d | γ_l^p |
| Water | 72.8 | 21.8 | 51.0 |
| Ethylene glycol | 48.0 | 29.0 | 19.0 |

326

327 **Supplementary Table 8**] Surface energy of PCA/AP1.6 and WPM II MF.

| Sample membranes | Contact angle (°) | | Surface-energy components (mN/m) | | |
|---------------------|-------------------|--------------------|----------------------------------|--------------|--------------|
| | Water | Ethylene glycol | γ_s | γ_s^d | γ_s^p |
| PCA/AP1.6 MF | 6 | 10 | 84.3 | 2.5 | 81.8 |
| WPM II MF | 0 | 18 | 88.2 | 1.5 | 86.8 |

328

329

330 **Supplementary Table 9**] O/W emulsion separation permeance information of WPM II
 331 MF and high-performance membranes reported in open literatures²⁻²⁸.

| Membrane | Modificati on strategy | Model oil | Surfact ant | Pure water flux | Permeab ility ($L \cdot m^{-2}$ | Oil rejectio n (%) | Trans- memb rane | Referen ce |
|----------|---------------------------|--------------|----------------|-----------------------|--|--------------------------|------------------------|---------------|
|----------|---------------------------|--------------|----------------|-----------------------|--|--------------------------|------------------------|---------------|

| | | | | h-1) | pressu re (bar) | | | |
|-------------------------------------|-------------------|---------------|-------------|-----------|-----------------------|------|------|----|
| PVDF/TA- PEI/Ti ⁴⁺ | Coating | Pump oil | SDS | 6736 | 3139 | 99.9 | 0.5 | 2 |
| PVDF- PG/PEI | Coating | Toluene | SDS | 1333 | 1053 | 98.4 | 0.1 | 3 |
| PA@PEI/P VDF | Coating | Toluene | Tween 80 | / | 1343 | 99.1 | 0.15 | 4 |
| Janus PVDF | Pray- coating | Toluene | Tween 80 | / | 2060 | 94 | 1 | 5 |
| HNTs@PV DF@PDA/ PSBMA | Coating | Soybean oi | SDS | / | 2365 | 99.8 | 0.85 | 6 |
| UF-T/C | Coating | Toluene | Tween 80 | 7900 | 2000 | 99.5 | 0.9 | 7 |
| CNT@PD A-ZT | Nano- assembly | n- Hexane | SDS | 3360 | 1880 | 99.6 | 0.5 | 8 |
| MF-DA/TA | Coating | Toluene | Tween 80 | 1350 0 | 2100 | 99.6 | 0.09 | 9 |
| GO/LDH | LBL | Decane | | | 1900 | 93 | 1 | 10 |
| Cu ²⁺ /alginat e/PVDF | Coating | Crude oil | SDS | 1600 | 1230 | 99.8 | 1 | 11 |
| PP/PDA- PVP | Coating | SO | DC193 | 440 | 268 | 98 | 1 | 12 |
| PVDF/CS& DA | Coating | PO | SDS | 201 | 171 | 99.7 | 0.1 | 13 |
| GA- APTES/PV | Coating | Toluene | Tween 80 | 1027 3 | 1000 | 99.5 | 0.9 | 14 |

| | | | | | | | | |
|----------------------|----------|-----------|-------|------|-------|-------|-----|----|
| DF | | | | | | | | |
| PK-g- | Coating | Toluene | SDS | 1820 | 1710 | 99.7 | 1 | 15 |
| PSBMA | | | | | | | | |
| SWCNT/P | Nano- | Industria | Tween | 7270 | 6060 | 99.99 | 0.5 | 16 |
| D/PEI | assembly | l oil | 80 | | | | | |
| Pal coated | Coating | kerosene | Tween | / | 477.7 | 99.6 | 0.8 | 17 |
| membrane | | | 80 | | | | | |
| PVDF-TA- | Coating | Glycerol | SDS | 2250 | 1800 | 99 | 0.6 | 18 |
| SP | | | | | | | | |
| loess- | Coating | Petroleu | Tween | 7000 | 910.4 | 99.6 | 1 | 19 |
| coated | | m ether | 80 | | | | | |
| PVDF | | | | | | | | |
| PVDF@pD | Coating | Dichloro | Tween | / | 572 | 98 | 0.8 | 20 |
| A@SiO ₂ | | methane | 80 | | | | | |
| MF-T/K | Coating | Toluene | Tween | / | 2580 | 99.2 | 1 | 21 |
| | | | 80 | | | | | |
| PVDF- | Coating | Toluene | Tween | 6364 | 2500 | 99.6 | 1 | 22 |
| TAAP | | | 80 | | | | | |
| TA- | Coating | Toluene | Tween | 1038 | 2650 | 99.7 | 1 | 23 |
| APTES- | | | 20 | 4 | | | | |
| TEOS | | | | | | | | |
| TA- | Coating | Toluene | SDS | / | 2200 | 99 | 1 | 24 |
| APTES-Fe | | | | | | | | |
| PVDF- | Coating | Toluene | Tween | 1300 | 2700 | 99.5 | 1 | 25 |
| POSS- | | | 80 | 0 | | | | |
| NH ₂ /FPN | | | | | | | | |
| MF-C/A | Coating | Toluene | Tween | 1300 | 1300 | 99 | 1 | 26 |
| | | | 80 | 0 | | | | |
| Coating- | Coating | Toluene | / | / | 2750 | 99 | 1 | 27 |

deposited

copper

mesh

| | | | | | | | | |
|------------|----------------------|---------------------|-------------|-------------|------|------|------|--------------|
| chitin NFs | Vacuum- filtering | Toluene | Tween 80 | 2630 | 563 | 91 | 0.95 | 28 |
| WPM II | Coating | Petroleu m ether | Tween 80 | 1755 5.5 | 5635 | 99.6 | 1 | This work |

332

333 **Supplementary Table 10** | Mechanical properties of different membranes.

| Ionomer | E/MPa | TS/MPa | ϵ /% |
|--------------|-------|--------|---------------|
| Pristine MF | 1.53 | 23.72 | 39.87 |
| PCA/AP0.4 MF | 3.17 | 25.5 | 29.29 |
| WPM 0 MF | 5.63 | 27.52 | 26.57 |
| PCA/AP0.8 MF | 5.92 | 27.95 | 23.13 |
| WPM I MF | 6.81 | 30.25 | 21.5 |
| PCA/AP1.6 MF | 6.66 | 34.93 | 21.72 |
| WPM II MF | 7.69 | 36.47 | 21.31 |

334

335 **Reference**

336 1. Ohno, S., Hori, W., Hosokawa, M., Tatsuzawa, F. & Doi, M. Post-transcriptional silencing of chalcone
337 synthase is involved in phenotypic lability in petals and leaves of bicolor dahlia (*Dahlia variabilis*) 'Yuino'.
338 *Planta* **247**, 413-428 (2018).

339 2. Zhao, X. *et al.* Engineering superwetting membranes through polyphenol-polycation-metal
340 complexation for high-efficient oil/water separation: From polyphenol to tailored nanostructures. *J.*
341 *Membr. Sci.* **630**, 119310 (2021).

342 3. Zuo, C. *et al.* Co-deposition of pyrogallol/polyethyleneimine on polymer membranes for highly
343 efficient treatment of oil-in-water emulsion. *Sep. Pur. Tech.* **267**, 118660 (2021).

344 4. Zeng, X. *et al.* Fabrication of superhydrophilic PVDF membranes by one-step modification with eco-
345 friendly phytic acid and polyethyleneimine complex for oil-in-water emulsions separation. *Chemosphere*

346 **264**, 128395 (2021).

347 5. Zuo, J.-H. *et al.* Janus polyvinylidene fluoride membranes fabricated with thermally induced phase
348 separation and spray-coating technique for the separations of both W/O and O/W emulsions. *J. Membr.*
349 *Sci.* **595**, 117475 (2020).

350 6. Zhou, Y. *et al.* A modified TA-APTES coating: Endowing porous membranes with uniform, durable
351 superhydrophilicity and outstanding anti-crude oil-adhesion property via one-step process. *J. Membr.*
352 *Sci.* **618**, 118703 (2021).

353 7. Yang, X., Yan, L., Ma, J., Bai, Y. & Shao, L. Bioadhesion-inspired surface engineering constructing robust,
354 hydrophilic membranes for highly-efficient wastewater remediation. *J. Membr. Sci.* **591**, 117353 (2019).

355 8. Zhao, X. *et al.* Bioinspired synthesis of polyzwitterion/titania functionalized carbon nanotube
356 membrane with superwetting property for efficient oil-in-water emulsion separation. *J. Membr. Sci.* **589**,
357 117257 (2019).

358 9. Yang, X., Yan, L., Wu, Y., Liu, Y. & Shao, L. Biomimetic hydrophilization engineering on membrane
359 surface for highly-efficient water purification. *J. Membr. Sci.* **589**, 117223 (2019).

360 10. Zhao, X., Jia, N., Cheng, L., Liu, L. & Gao, C. Metal-polyphenol coordination networks: Towards
361 engineering of antifouling hybrid membranes via in situ assembly. *J. Membr. Sci.* **563**, 435-446 (2018).

362 11. Jiang, J. *et al.* Antifouling and antimicrobial polymer membranes based on bioinspired polydopamine
363 and strong hydrogen-bonded poly(*n*-vinyl pyrrolidone). *ACS Appl. Mater. Inter.* **5**, 12895-12904 (2013).

364 12. Zhang, G. *et al.* Bio-inspired underwater superoleophobic PVDF membranes for highly-efficient
365 simultaneous removal of insoluble emulsified oils and soluble anionic dyes. *Chem. Eng. J.* **369**, 576-587
366 (2019).

367 13. Yang, X., Sun, H., Pal, A., Bai, Y. & Shao, L. Biomimetic silicification on membrane surface for highly
368 efficient treatments of both oil-in-water emulsion and protein wastewater. *ACS Appl. Mater. Inter.* **10**,
369 29982-29991 (2018).

370 14. Gao, S. J., Zhu, Y. Z., Zhang, F. & Jin, J. Superwetting polymer-decorated SWCNT composite ultrathin
371 films for ultrafast separation of oil-in-water nanoemulsions. *J. Mater. Chem. A* **3**, 2895-2902 (2015).

372 15. Zhang, L., Lin, Y., Cheng, L., Yang, Z. & Matsuyama, H. A comprehensively fouling- and solvent-
373 resistant aliphatic polyketone membrane for high-flux filtration of difficult oil-in-water micro- and
374 nanoemulsions. *J. Membr. Sci.* **582**, 48-58 (2019).

375 16. Cao, J. *et al.* Self-assembled MOF membranes with underwater superoleophobicity for oil/water

376 separation. *J. Membr. Sci.* **566**, 268-277 (2018).

377 17. Li, R. *et al.* Inkjet printing assisted fabrication of polyphenol-based coating membranes for oil/water
378 separation. *Chemosphere* **250**, 126236 (2020).

379 18. Sun, Y. *et al.* Surface hydrophilic modification of PVDF membranes based on tannin and zwitterionic
380 substance towards effective oil-in-water emulsion separation. *Sep. Pur. Tech.* **234**, 116015 (2020).

381 19. Xie, A. *et al.* Photo-Fenton self-cleaning membranes with robust flux recovery for an efficient
382 oil/water emulsion separation. *J. Mater. Chem. A* **7**, 8491-8502 (2019).

383 20. Cui, J. *et al.* Bio-inspired fabrication of superhydrophilic nanocomposite membrane based on surface
384 modification of SiO₂ anchored by polydopamine towards effective oil-water emulsions separation. *Sep.*
385 *Pur. Tech.* **209**, 434-442 (2019).

386 21. Wang, Z. *et al.* One-step transformation of highly hydrophobic membranes into superhydrophilic
387 and underwater superoleophobic ones for high-efficiency separation of oil-in-water emulsions. *J. Mater.*
388 *Chem. A* **6**, 3391-3396 (2018).

389 22. Yang, X. *et al.* Mussel-/diatom-inspired silicified membrane for high-efficiency water remediation. *J.*
390 *Membr. Sci.* **597**, 117753 (2020).

391 23. Wang, Z. *et al.* Investigating and significantly improving the stability of tannic acid (TA)-
392 aminopropyltriethoxysilane (APTES) coating for enhanced oil-water separation. *J. Membr. Sci.* **593**,
393 117383 (2020).

394 24. Zhao, Y. *et al.* Ultra-robust superwetting hierarchical membranes constructed by coordination
395 complex networks for oily water treatment. *J. Membr. Sci.* **627**, 119234 (2021).

396 25. Yang, X. *et al.* Mussel-inspired structure evolution customizing membrane interface hydrophilization.
397 *J. Membr. Sci.* **612**, 118471 (2020).

398 26. Lu, J. *et al.* Photocatalytically active superhydrophilic/superoleophobic coating. *ACS Omega* **5**,
399 11448-11454 (2020).

400 27. Wang, Z. *et al.* Separation of caustic nano-emulsions and macromolecular conformations with
401 nanofibrous membranes of marine chitin. *ACS Appl. Mater. Inter.* **11**, 8576-8583 (2019).

402 28. Zhou, L. *et al.* Multifunctional filtration membrane with anti-viscous-oils-fouling capacity and
403 selective dyes adsorption ability for complex wastewater remediation. *J. Hazard. Mater.* **413**, 125379
404 (2021).

405

